








RESEARCH PAPER

PHOSPHATE1-mediated phosphate translocation from roots to shoots regulates floral transition in plants

Senhuan Dai¹, Huiying Chen¹, Yutao Shi¹, Xinlong Xiao² , Lei Xu³ , Cheng Qin¹ , Yiyong Zhu⁴ , Keke Yi³ ,
Mingguang Lei¹ , and Houqing Zeng^{1,*} 

¹ College of Life and Environmental Sciences, Hangzhou Normal University, Hangzhou 311121, China

² Shanghai Center for Plant Stress Biology, CAS Center for Excellence in Molecular Plant Sciences, Chinese Academy of Sciences, Shanghai, China

³ State Key Laboratory of Efficient Utilization of Arid and Semi-arid Arable Land in Northern China, Institute of Agricultural Resources and Regional Planning, Chinese Academy of Agricultural Sciences, Beijing, China

⁴ Jiangsu Collaborative Innovation Center for Solid Organic Waste Resource Utilization, College of Resources and Environment Sciences, Nanjing Agricultural University, Nanjing 210095, China

* Correspondence: zenghq@hznu.edu.cn

Received 15 December 2023; Editorial decision 10 May 2024; Accepted 15 May 2024

Editor: Guohua Xu, Nanjing Agricultural University, China

Abstract

Phosphorus nutrition has been known for a long time to influence floral transition in plants, but the underlying mechanism is unclear. Arabidopsis phosphate transporter PHOSPHATE1 (PHO1) plays a critical role in phosphate translocation from roots to shoots, but whether and how it regulates floral transition is unknown. Here, we show that knockout mutation of *PHO1* delays flowering under both long- and short-day conditions. The late flowering of *pho1* mutants can be partially rescued by Pi supplementation in rosettes or shoot apices. Grafting assay indicates that the late flowering of *pho1* mutants is a result of impaired phosphate translocation from roots to shoots. Knockout mutation of *SPX1* and *SPX2*, two negative regulators of the phosphate starvation response, partially rescues the late flowering of *pho1* mutants. *PHO1* is epistatic to *PHO2*, a negative regulator of *PHO1*, in flowering time regulation. Loss of *PHO1* represses the expression of some floral activators, including *FT* encoding florigen, and induces the expression of some floral repressors in shoots. Genetic analyses indicate that at least jasmonic acid signaling is partially responsible for the late flowering of *pho1* mutants. In addition, we find that rice *PHO1;2*, the homolog of *PHO1*, plays a similar role in floral transition. These results suggest that *PHO1* integrates phosphorus nutrition and flowering time, and could be used as a potential target in modulating phosphorus nutrition-mediated flowering time in plants.

Keywords: Arabidopsis, flowering, jasmonic acid signaling, pathway, PHO1, phosphorus.

Introduction

Phosphorus (P) is an essential macronutrient acting as a major structural constituent of fundamental macromolecules, such as nucleic acids and phospholipids in plants. Due to the

adsorption, precipitation, or conversion to organic forms, most P in soils is not available to plants (Veneklaas *et al.*, 2012). Low phosphate (Pi) in soils is becoming a limiting factor for crop

productivity worldwide, and substantial use of Pi fertilizers is the main solution to this problem. However, relying on Pi fertilizers to maintain or increase crop yield is challenging, because reserves of Pi rock (the primary source of Pi fertilizers) are finite, the cost of Pi fertilizers is high, and Pi overuse leads to environmental problems such as eutrophication (Sattari *et al.*, 2016). Therefore, it is necessary to increase the ability of plants to acquire Pi from soils and optimize the internal use of Pi to achieve a high yield in order to cut down the input of Pi fertilizers. To maintain internal Pi homeostasis under low Pi conditions, plants have evolved a series of adaptive strategies, including enhancement of Pi acquisition by plant roots, coordination of the translocation and allocation of Pi in different organs, and remobilization of Pi from old tissues to young tissues (Madison *et al.*, 2023). Many genes have been functionally identified to regulate Pi homeostasis and Pi starvation responses in plants (Lopez-Arredondo *et al.*, 2014; Lu *et al.*, 2023). PHOSPHATE STARVATION RESPONSE1 (PHR1) and its close homolog PHR1-like 1 (PHL1) are MYB-coiled-coil (MYB-CC) transcription factors playing a central role in regulating the expression of a group of Pi starvation-responsive (PSR) genes (Bustos *et al.*, 2010). In Arabidopsis, SPX1 and SPX2 interact with PHR1 and negatively regulate the transcriptional activity of PHR1 (Puga *et al.*, 2014).

PHOSPHATE 1 (PHO1), encoding an SPX-EXS protein, is predominantly expressed in root stelar cells and plays a major role in root-to-shoot translocation of Pi by loading Pi into the xylem of roots (Poirier *et al.*, 1991). The homologs of PHO1 in other plants, such as OsPHO1;2 in rice and SlPHO1;1 in tomato, also function in mediating Pi translocation from roots to shoots (Secco *et al.*, 2010; Zhao *et al.*, 2019). PHO1 possesses a hydrophilic region harboring an SPX domain in the N-terminus, four transmembrane α -helices in the middle region, and a hydrophobic region containing an EXS domain in the C-terminus. The SPX domain of PHO1 is involved in the binding of inositol phosphates (Wild *et al.*, 2016; Jung *et al.*, 2018), and the EXS domain is essential for the Pi export activity of PHO1 (Wege *et al.*, 2016). In Arabidopsis, genetic inactivation of PHO1 results in severe growth retardation, and *pho1* mutants display low Pi content in shoots (Poirier *et al.*, 1991). Interestingly, *pho1* leaves accumulate significantly higher jasmonic acid (JA)/JA-isoleucine (JA-Ile) and exhibit increased resistance to herbivores when compared with the wild type (WT); the phenotypes of the *pho1* mutant associated with Pi deficiency are impaired by blocking JA biosynthesis or the signaling pathway (Khan *et al.*, 2016). In addition, PHO1-mediated Pi flux functions in plant seed development by delivering Pi from the maternal tissues to the filial tissues (Vogiatzaki *et al.*, 2017; Che *et al.*, 2020; Ma *et al.*, 2021). PHO1 is also involved in Arabidopsis stomatal response to abscisic acid (ABA) and ABA-mediated seed germination (Zimmerli *et al.*, 2012; Huang *et al.*, 2017). Notably, PHO1 is regulated at both the transcriptional and protein levels to avoid either Pi overaccumulation or Pi deficiency in the

aerial tissues. PHO1 is negatively regulated at the transcriptional level by WRKY transcription factors, such as WRKY6 and WRKY42 (Chen *et al.*, 2009). On the other hand, PHO1 abundance is modulated at the protein level via its degradation in the endomembrane by involving a ubiquitin-conjugating E2 enzyme, PHOSPHATE 2 (PHO2). A knockout mutant of *PHO2* accumulates high levels of Pi and exhibits Pi toxicity in shoots due to enhanced Pi uptake in roots and increased Pi translocation from roots to shoots in Arabidopsis (Delhaize and Randall, 1995). PHO2 is post-transcriptionally repressed by a specific miRNA, miR399, which is induced by Pi starvation with the involvement of PHR1 (Aung *et al.*, 2006; Bari *et al.*, 2006). Thus, under Pi deficiency, the action of PHO2 on PHO1 and on the Pi transporter PHT1 is decreased, leading to the benefit of Pi acquisition and translocation in plants (T.Y. Liu *et al.*, 2012; Huang *et al.*, 2013).

Flowering plants respond to environmental and endogenous signals to determine the timing of the transition from vegetative growth to reproductive growth. Appropriate flowering time is essential for reproductive success, which enables the completion of seed development under favorable environmental conditions. Flowering time is tightly regulated by environmental stimuli, such as changes in the day length, temperature, and nutrient status, and endogenous signals, such as hormones and plant age (Kim *et al.*, 2009; Andrés and Coupland, 2012; Wang, 2014; Cho *et al.*, 2017). The strict control of flowering is conferred by a network of genetic pathways, including photoperiod, vernalization, gibberellic acid (GA), autonomous, thermosensory, and age-dependent pathways (Srikanth and Schmid, 2011; Andrés and Coupland, 2012; Wang, 2014). The floral activators FLOWERING LOCUS T (FT) and SUPPRESSOR OF CONSTANS OVEREXPRESSION 1 (SOC1) and the floral repressor FLOWERING LOCUS C (FLC) converge in various flowering pathways, where FT and SOC1 activate the transcription of floral meristem identity genes that are related to floral organ formation, such as *APETALA 1* (*AP1*) and *LEAFY* (*LFY*) (Srikanth and Schmid, 2011; Andrés and Coupland, 2012; Kinoshita and Richter, 2020). FT in Arabidopsis and its homologs in other plants have been identified to be the long-sought florigen, a long-distance mobile floral stimulus moving from leaves to the shoot apex to induce the formation of flowers (Kojima *et al.*, 2002; Corbesier *et al.*, 2007; Tamaki *et al.*, 2007; Zhu *et al.*, 2016). The photoperiodic pathway regulates flowering by integrating inputs from circadian clock-controlled GIGANTEA (GI) and photoreceptors, and CONSTANS (CO), a B-box zinc-finger transcription factor, functions as the central regulator in this pathway by inducing the expression of *FT* (Shim *et al.*, 2017). The protein stability of CO is positively regulated by the blue light receptors cryptochrome 1 (CRY1) and CRY2, and the red light/far-red light receptor phytochrome A (phyA), but is negatively regulated by phyB (Valverde *et al.*, 2004). FLC, a MADS-box transcription factor, antagonizes the GA and photoperiod pathways by repressing flowering promoters, such as

FT and *SOC1* (Searle *et al.*, 2006; Sharma *et al.*, 2020). The transcription of *FLC* is epigenetically down-regulated through the vernalization and autonomous pathways at ambient temperatures, allowing flowering during long days (Berry and Dean, 2015). SHORT VEGETATIVE PHASE (SVP), another MADS-box transcription factor, is a floral suppressor acting in ambient temperature-responsive flowering, since *svp* mutants displayed temperature-insensitive early flowering over a range of temperatures (Lee *et al.*, 2007). SVP inhibits the expression of *FT* by directly binding to its promoter region. The transcript level of *SVP* does not change dramatically with temperature, but the protein abundance and stability of SVP are affected by temperature (Lee *et al.*, 2007, 2013).

External nutrient levels including those of nitrogen (N) and P have been demonstrated to influence the time of floral transition in plants (Zhang *et al.*, 2022). In *Arabidopsis*, low N conditions have been known to accelerate flowering by reducing the protein phosphorylation level of the FLOWERING BHLH 4 (FBH4) transcription factor, which is an activator of the CO/FT photoperiodic pathway (Sanagi *et al.*, 2021). It has also been shown that flowering time is delayed by P deficiency in plants, such as tomato and subterranean clover (*Trifolium subterraneum*) (Menary and Staden, 1976; Rossiter, 1978). P fertilizers can promote flowering in plants, such as rice (Ye *et al.*, 2019), and the alpine *Gnaphalium supinum* (Petraglia *et al.*, 2014). In *Arabidopsis*, both miR399b-overexpressing plants and *pho2* mutants that overaccumulate Pi in shoots exhibit early flowering phenotypes (Kim *et al.*, 2011). These findings suggest that flowering time is modulated by Pi availability. However, the molecular mechanisms underlying the linkage between Pi homeostasis and flowering remain largely unknown.

In this work, we show that knockout mutation of *PHO1* delays flowering in *Arabidopsis*, which can be partially rescued by Pi supplementation in rosettes or shoot apices. Grafting assay indicates that late flowering of *pho1* mutants results from impaired Pi translocation from roots to shoots. Loss of *PHO1* affects the expression of a group of flowering time genes, including *FT* and *TSF*. Genetic analyses suggest that the late flowering of *pho1* mutants depends on FT and SVP, and JA signaling is responsible for the late flowering of *pho1* mutants. In addition, the PHO1-mediated flowering regulation is conserved in other plants such as rice. Our results suggest that *PHO1* is an important gene in the connection between P nutrition and flowering time in plants.

Materials and methods

Plant materials and growth conditions

Arabidopsis thaliana Columbia-0 (Col-0) was used as the WT in all experiments and for genetic transformation. The mutant alleles used were *pho1* (SAIL_423_E04), *pho1-2* (CS8507), *pho2* (SAIL_47_E01) (Xiao *et al.*, 2022), *phr1* (SALK_067629) (Sun *et al.*, 2016), *phl1* (SALK_079505), *phrl* *phl1* (Bustos *et al.*, 2010), *ft-10* (GABI_290E08), *soc1-2* (SALK_138131), *flc-3*, *co-9* (SAIL_24_H04), *svp-41*, *jar1-1* (Huang *et al.*, 2021), *coi1-2*

(Zhai *et al.*, 2015), and *spx1 spx2* (Puga *et al.*, 2014). Transgenic plants 35S:*FT*, *SUC2:FT*, *KNAT1:FT*, *SUC2:FT-GFP*, and *SUC2:FT-9myc* were described previously (L. Liu *et al.*, 2012; Zhu *et al.*, 2016). Double or triple mutants *pho1 pho2*, *pho1 ft-10*, *pho1 co-9*, *pho1 flc-3*, *pho1 svp-41*, *pho1 soc1-2*, *pho1 coi1-2*, *pho1 35S:FT*, *pho1 SUC2:FT*, *pho1 KNAT1:FT*, *pho1 SUC2:FT-GFP*, *pho1 SUC2:FT-9myc*, and *pho1 spx1 spx2* were generated by genetic crossing. pPHO1:PHO1-GFP (green fluorescent protein) was constructed by cloning the promoter sequences (2.0 kb) and the genomic sequences of PHO1 (without the stop codon) into the pCAMBIA1300-GFPc vector. Complementation lines (pPHO1:PHO1-GFP/*pho1*) were generated by the transformation of *pho1* with *Agrobacterium* carrying the pPHO1:PHO1-GFP vector (Xiao *et al.*, 2022). pPHO1:GUS (β -glucuronidase) lines were obtained by cloning a 1.6 kb region upstream of the transcriptional start site of PHO1 into the pCAMBIA1300-GUS-plus vector. Transgenic plants were created using the floral dip method (Clough and Bent, 1998) and screened by hygromycin added to half-strength Murashige and Skoog (1/2 MS) plates.

Arabidopsis seeds were sterilized by using 10% NaClO for 10 min and stored in sterile water at 4 °C for 48 h for stratification, followed by germination at 22 °C in 1/2 MS medium (pH 5.7) with 1.5% sucrose and 1% (w/v) agar. Seven-day-old seedlings were then transplanted into soil and grown in a growth room at 22 °C/20 °C with a 16 h light/8 h dark regime [long-day (LD) conditions], or with a 8 h light/16 h dark regime [short-day (SD) conditions]. The light intensity was $\sim 100 \mu\text{mol m}^{-2} \text{s}^{-1}$.

Arabidopsis hydroponic culture was conducted according to Zeng *et al.* (2018a). For low Pi or Pi deficiency treatment, KH_2PO_4 was replaced by K_2SO_4 . For phenotype observation of mutants under hydroponic culture, 1-week-old plants grown under normal hydroponic conditions were transferred to hydroponic solutions with different concentrations of Pi.

To generate rice *pho1;2* knockout plants, a 20 bp gene-specific spacer sequence of *PHO1;2* (Os02g56510) was inserted into the single guide RNA (sgRNA)/Cas9 [clustered regularly interspaced palindromic repeats (CRISPR)-associated protein 9] construct. The knockout construct was introduced into *Agrobacterium tumefaciens* strain EHA105, and Shishoubaimao (SSBM) (*Oryza sativa* ssp. *japonica*) was used for rice genetic transformation. T₀ transgenic lines were analyzed by sequencing. Homozygous transgenic lines were selected and used for phenotypic observation. Primers used in this assay are listed in Supplementary Table S1.

Flowering time analysis

Flowering time was scored as the total number of rosette leaves at the bolting stage when the main stem had reached a height of ~ 0.5 cm. The number of days at bolting was also measured. At least 15 plants were examined for each genotype. The flower buds of plants were observed every day.

Determination of Pi concentration

The Pi concentration in plants was determined according to Zeng *et al.* (2018b). About 0.4 g of fresh tissue frozen in liquid nitrogen was ground into fine powder, and it was then suspended in extraction buffer (10 mM Tris, 1 mM EDTA, 100 mM NaCl, and 1 mM β -mercaptoethanol, pH 8.0) at a ratio of 1 mg of FW of the sample to 10 μl of extraction buffer. A total of 110 μl of sample suspension was mixed with 990 μl of 1% glacial acetic acid and then incubated at 42 °C for 30 min. Then, the suspension was centrifuged at 12 000 g for 10 min and 1.0 ml of the supernatant was used for the quantitative determination of Pi. A reaction mixture containing 2.0 ml of Pi determination solution [0.34% $(\text{NH}_4)_6\text{Mo}_7\text{O}_{24}\cdot 4\text{H}_2\text{O}$, 0.46M H_2SO_4 , and 1.4% ascorbic acid] and 1.0 ml of supernatant was incubated at 42 °C for 20 min. Then, it was cooled to room temperature, and the absorbance at 820 nm was measured using a UV-Vis spectrometer (Thermo Scientific BioMate 3S).

Inorganic orthophosphate staining assay

Inorganic orthophosphate staining assay (IOSA) was performed according to Guo *et al.* (2024). Arabidopsis seedlings (roots and shoots) were collected and washed with tap water. Samples were then stained with an adequate amount of IOSA detection buffer (IDB) (including 0.81 mM ammonium molybdate, 0.15 mM potassium antimonyl tartrate, 0.19 M sulfuric acid, and 1.7 M L-ascorbate) for 30–60 min under vacuum treatment. IDB was removed, and an appropriate amount of fixing buffer B was added to immerse all the samples for 30 min under vacuum treatment. Fixing buffer B was removed and an appropriate amount of discoloring buffer C was added to immerse all plants for several hours until all the chlorophyll of the samples was removed. After that, samples were transferred to a new tube containing clearing buffer D for 1–3 h, and then samples were photographed.

Anthocyanin quantification

Fresh tissue frozen with liquid nitrogen was ground into powder with steel balls in a 1.5 ml centrifuge tube. A 1.0 ml aliquot of extraction solution (80% methanol, 0.5% hydrochloric acid, 19.5% H₂O) was added into the tube and an ultrasonic treatment at 40 Hz was conducted for 15 min. Each tube was centrifuged at 4 °C for 10 min at 5000 g. After that, 300 µl of supernatant was mixed with 150 µl of trichloromethane and 150 µl of water, and centrifuged at 4 °C for 10 min at 5000 g. Subsequently, supernatant was used to measure the absorbance at 535 nm and at 650 nm. Absorption values (A_{535} minus A_{650}) were used to determine anthocyanin content. Three biological replicates were included for measurement for each sample.

β-Glucuronidase staining

Histochemical detection of GUS activity was performed with 5-bromo-4-chloro-3-indolyl β-D-glucuronic acid (X-Gluc) as a substrate. Seedlings were infiltrated with ice-cold 90% (v/v) acetone for 20 min on ice and washed three times with ultrapure water. Seedlings were then inoculated with GUS staining solution [100 mM Na₂HPO₄, pH 7.0, 10 mM Na₂EDTA, 1.0 mM potassium ferrocyanide, 1.0 mM potassium ferricyanide, 0.5% (v/v) Triton X-100, 20% (v/v) methanol, and 0.5 mg ml⁻¹ X-Gluc] under vacuum conditions, and stained at 37 °C overnight. Chlorophyll of the samples was cleared by using 70% (v/v) ethanol. An optical stereomicroscope was used for the observation of GUS staining.

Grafting

Arabidopsis seeds were sown on a medium [1/2 MS, 2% (w/v) agar, 1.5% (w/v) sucrose] under SD conditions for 4–5 d. The hypocotyl of the seedling was vertically cut in the middle using a sharp razor blade, and the scion was quickly moved to the target rootstock. The scion and rootstock were firmly squeezed together with the assistance of an anatomical microscope (Phoenix Optics Group Co., Ltd, China). The Petri dishes were vertically aligned in a growth room under LD conditions. Two days after surgery, the scion and rootstock were joined. Samples without an appropriate connection were discarded. Adventitious roots on the scions were removed with Vannas spring scissors. Well-grafted seedlings with two true leaves were transplanted to the soil. The cut edge was left above the soil surface and was checked daily. Adventitious roots were immediately removed once they had emerged.

RNA-sequencing analysis

Shoots of 20-day-old Col-0 and *pho1* seedlings treated with KCl (pH 7) and KH₂PO₄ (pH 7) sprays for 11 d were harvested for total RNA extraction using TRIzol® reagent according to the manufacturer's instructions. Genomic DNA in the RNA was removed using DNase I (TaKaRa, Dalian, China). RNA quality was determined by a 2100 Bioanalyser (Agilent) and quantified using the ND-2000 (NanoDrop Technologies).

Only high-quality RNA sample [OD₂₆₀/OD₂₈₀=1.8–2.2, OD₂₆₀/OD₂₃₀ ≥2.0, RNA integrity number (RIN) ≥6.5, 28S:18S ≥1.0, concentration >1 µg µl⁻¹] was used for the subsequent construction of the RNA-sequencing (RNA-seq) library by using the TruSeq™ RNA sample preparation kit from Illumina (San Diego, CA, USA) according to the manufacturer's instructions. High-throughput sequencing was performed on the Illumina HiSeq×10/NovaSeq 6000 sequencer. The raw paired-end reads were trimmed and quality controlled by SeqPrep (<https://github.com/jstjohn/SeqPrep>) and Sickle (<https://github.com/najoshi/sickle>) with default parameters. Next, clean reads were separately aligned to the reference Arabidopsis genome TAIR10 by using HISAT2 software (Kim *et al.*, 2015). The mapped reads of each sample were assembled by StringTie in a reference-based approach (Pertea *et al.*, 2015). To identify differentially expressed genes (DEGs) between two treatments or genotypes, the estimated gene abundance was measured in terms of the transcripts per million reads (TPM). RSEM (<http://deweylab.biostat.wisc.edu/rsem/>) was used to quantify gene abundances (Li and Dewey, 2011). Only the genes with a log₂ fold change ≥1 or ≤ -1, and an adjusted *P*-value ≤0.05 were considered as significantly DEGs. The RNA-seq datasets were deposited in the NCBI Sequence Read Archive (SRA) with accession number PRJNA1014575.

Gene ontology (GO) enrichment analysis of DEGs was conducted by using Goatools (Klopfenstein *et al.*, 2018). Enriched GO terms with an adjusted *P*-value ≤0.05 were regarded as significantly enriched.

Quantitative reverse transcription-PCR analysis

Total RNA was extracted with the Ultrapure RNA Kit (CWBI, Beijing, China), and then the cDNA was synthesized with total RNA using reverse transcriptase (HiScript®III All-in-one RT SuperMix Perfect for qPCR) (Vazyme, Nanjing, China) according to the manufacturer's instruction. Real-time quantitative reverse transcription-PCR (qRT-PCR) was performed with Taq Pro Universal SYBR qPCR Master Mix (Vazyme, Nanjing, China), and amplification was real-time monitored on a real-time PCR system (QuantStudio 3, Applied Biosystems). PCR efficiency was determined by a series of 5-fold dilutions of cDNAs, and the calculated efficiency of all primers was ~2.0. All reactions were run in triplicate together with controls that did not contain template in the reverse transcription. Relative expression levels of genes were normalized to those of two internal control genes, *ACTIN2* (At3g18780) and *TUBULIN2* (At5g62690), and presented as 2^{-ΔΔCT} to simplify the presentation of data (Zeng *et al.*, 2022). Sequences of gene-specific primers are listed in Supplementary Table S1.

Yeast two-hybrid assay

The coding sequence of FT was amplified from cDNA and cloned into pGBKT7 to produce the BD-FT vector. The coding sequence of PHO1 was amplified from cDNA and cloned into pGADT7 to produce the AD-PHO1 vector. After co-transformation of AD-PHO1 and BD-FT, as well as their corresponding empty vectors, the transformed yeast cells were grown on SD medium lacking Trp and Leu (SD-Trp/-Leu), and SD medium lacking His, Trp, and Leu (SD-His/-Trp/-Leu), respectively. The yeast two-hybrid (Y2H) assay was performed using the Yeastmaker Yeast Transformation System 2 in accordance with the manufacturer's instructions (Clontech, Palo Alto, CA, USA).

Results

Knockout mutation of *PHO1* results in late flowering in Arabidopsis

Two individual *pho1* mutants were used to examine the flowering phenotype; one is a T-DNA insertion mutant in the fifth intron

(Dong *et al.*, 2019) and the other is a point mutation leading to the synthesis of a truncated PHO1 protein (Hamburger *et al.*, 2002) (Supplementary Fig. S1). These two *pho1* mutants showed significantly late flowering phenotypes under LD conditions when compared with the WT (Col-0) (Fig. 1A). The rosette leaf number (RLN) at bolting and the days at bolting indicated that *pho1* mutants flowered significantly later than WT plants under LD conditions (Fig. 1B, C). Under SD conditions, the days at bolting of *pho1* mutants were dramatically higher than that of the WT, although the RLN at bolting was lower than that of the WT

(Fig. 1D–F). These results suggest that *pho1* mutants exhibit late flowering under both LD and SD conditions.

To confirm that the late flowering in these mutants is due to the mutation in *PHO1*, we analyzed the flowering phenotype by using the complementation lines of *pho1* (*pPHO1:PHO1-GFP/pho1*#4, #5) (Xiao *et al.*, 2022). The late flowering phenotype in *pho1* was rescued by complementation with the native promoter-driven genomic DNA fragment of *PHO1* (Fig. 1G–I). These results indicate that *PHO1* plays a positive role in floral transition.

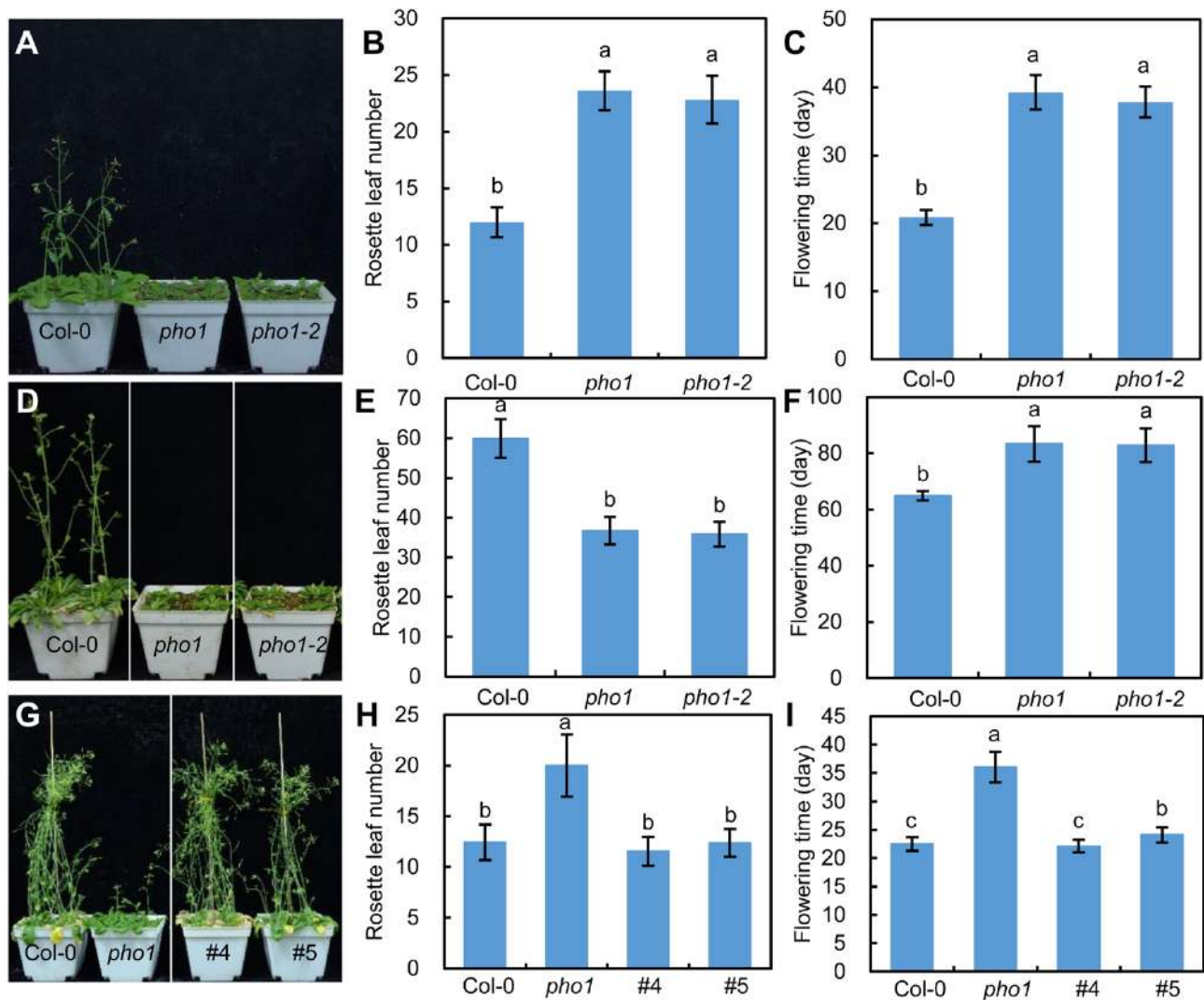


Fig. 1. Late flowering phenotypes of *pho1* mutants under both long-day (LD) and short-day (SD) conditions. (A) *pho1* and *pho1-2* plants exhibits late flowering phenotypes under LDs. The photo was taken after growing for 44 d under LD conditions. Flowering times were measured by counting rosette leaf number at bolting (B) and the days at bolting (C) ($n=16$, \pm SD). (D) *pho1* and *pho1-2* plants exhibits late flowering phenotypes under SDs. The photo was taken after growing for 78 d under SDs. Flowering times were measured by counting rosette leaf number at bolting (E) and the days at bolting (F) ($n=16$, \pm SD). (G) Late flowering phenotype of *pho1* mutants is rescued by complementation with ProPHO1:PHO1-GFP #4 and #5 are transgenic lines complemented with ProPHO1:PHO1-GFP in the background of the *pho1* mutant. The photo was taken after growing for 47 d under LDs. (H) Rosette leaf number at bolting, and days at bolting (I) for Col-0, *pho1*, #4, and #5 plants ($n=16$, \pm SD). Different letters indicate that values are significantly different at $P<0.05$ (Student's *t*-test).

Because the RLN of *pho1* mutants at bolting under SD was lower than that of the WT, we hypothesized that the knockout mutation may affect the leaf initiation. By measuring the RLN of the WT and *pho1* mutants during their growth period, we found that the leaf initiation rate of *pho1* mutants was significantly decreased under both LD and SD conditions (Supplementary Fig. S2). These results suggest that knockout mutation of *PHO1* influences the leaf initiation rate. Under SDs, the leaf initiation rate of *pho1* mutants was dramatically lower than that of the WT (Supplementary Fig. S2B); this may be the reason why *pho1* mutants flower later but had lower RLN under SD conditions.

Late flowering phenotype of *pho1* can be partially rescued by Pi supplementation in the shoot

Given that *PHO1* plays an important role in Pi homeostasis by mediating Pi translocation from roots to shoots (Hamburger *et al.*, 2002), it is reasonable to wonder whether the late flowering phenotype of *pho1* is associated with Pi nutrition. Thus, we conducted hydroponic culture with different Pi concentrations and analyzed the flowering phenotype of *pho1* mutants. Under normal Pi (0.25 mM), high Pi (2.0 mM), or low Pi (0.02 mM) conditions, the late flowering phenotype of *pho1* mutants was shown to be consistent (Supplementary Fig. S3A–C), suggesting that the alteration of flowering time by *PHO1* mutation occurs irrespective of the external Pi concentration in the growth medium.

Considering that Pi translocation from roots to shoots is impaired and that the shoot Pi concentration is much lower in *pho1* mutants (Hamburger *et al.*, 2002; T.Y. Liu *et al.*, 2012), we speculated that the late flowering phenotype of *pho1* mutants may be caused by Pi starvation in the shoot. Therefore, we supplemented Pi in the rosettes of *pho1* mutants by spraying KH_2PO_4 solution (10 mM, pH 7.0). After spraying with Pi solution for 15 d in *pho1* mutants, the growth was promoted, the shoot biomass was significantly increased, and the Pi concentration of leaves was higher when compared with those of *pho1* plants under water or KCl spray (Fig. 2A–C). For WT plants, Pi spray increased leaf Pi concentration but had a negative effect on plant growth when compared with the control treatment of KCl spray (Fig. 2B). The flowering time of the WT was not changed by the application of Pi or KCl spray, but the flowering time of *pho1* mutants was accelerated by Pi spray (Fig. 2D–F). These results reveal that Pi supplementation in rosettes by Pi spray could partially recover the late flowering phenotype of *pho1* mutants. Because flowers initiate at shoot apices, we then determined the Pi concentration in the shoot apices of the WT and *pho1* mutants, which were harvested by removing the cotyledons and all leaves >5 mm. By using the IOSA method to stain Pi, we found that there was less blue staining in the leaves and shoot apices of *pho1* when compared with the WT (Fig. 3A). The Pi concentration in the shoot apices of *pho1* was significantly lower than that of the WT, but it was

dramatically increased by the application of Pi spray in the rosette (Fig. 3B–D).

We further analyzed whether Pi supplementation at shoot apices has effects on *pho1* flowering by applying KH_2PO_4 solution at shoot apices. Similar to KH_2PO_4 application at mature leaves, KH_2PO_4 application at shoot apices also accelerated the flowering of *pho1* mutants when compared with the control of KCl application (Supplementary Fig. S4). However, KH_2PO_4 application at shoot apices had no significant effect on the flowering time of the WT. These results indicated that Pi supplementation at shoot apices partially rescues the late flowering phenotype of *pho1* mutants. We then wondered whether *PHO1* could be expressed at shoot apices and vascular tissue of leaves. By generating *pPHO1:GUS* transgenic lines and GUS staining, we found that *PHO1* was mainly expressed in the hypocotyl and roots of Arabidopsis seedlings, and in the stigma and peduncle during reproductive growth, but no distinct expression of *PHO1* was found in leaf vascular tissue (Supplementary Fig. S5). For the seedlings grown in soils, the expression of *PHO1* was detected in the shoot apices, but was not found in the mature leaves (Supplementary Fig. S5).

Based on the finding that the late flowering phenotype of *pho1* mutants is a result of the low Pi concentration in the shoot, we wondered whether low Pi treatment results in late flowering in the WT. We further analyzed the flowering time of the WT under various low Pi conditions (from moderately low Pi to extremely low Pi). Various low Pi treatments reduced the growth and the Pi concentration of WT plants, while the anthocyanin content was significantly increased by low Pi treatments (Fig. 4A–C). Interestingly, the flowering time of the WT was repressed by low Pi treatments, especially under extremely low Pi conditions (1/25 P and 1/50 P) (Fig. 4D, E).

Grafting experiments indicate that the late flowering of *pho1* results from Pi deficiency in shoots

To investigate whether the late flowering of *pho1* mutants results from defective shoots or roots, we performed a reciprocal micrografting experiment with WT and *pho1* mutant seedlings. When *pho1* shoot was used as a scion grafted onto WT rootstock, the growth retardation and Pi deficiency symptoms of *pho1* shoots were rescued to the level of the WT scion control (Fig. 5A). However, when *pho1* was used as the rootstock, the rosette sizes of *pho1* and WT scions were significantly smaller than those with a WT rootstock (Fig. 5A). These results indicate that *PHO1* function in the root is required for Pi translocation from roots to shoots, which is consistent with previous reports (Wege *et al.*, 2016). The grafting with WT rootstock accelerated the flowering time of the *pho1* scion, but the flowering time of the WT scion was delayed by the grafting with *pho1* rootstock (Fig. 5B–D). These results indicate that *PHO1* mutation in roots is necessary and sufficient for the late flowering phenotype of *pho1* mutants.

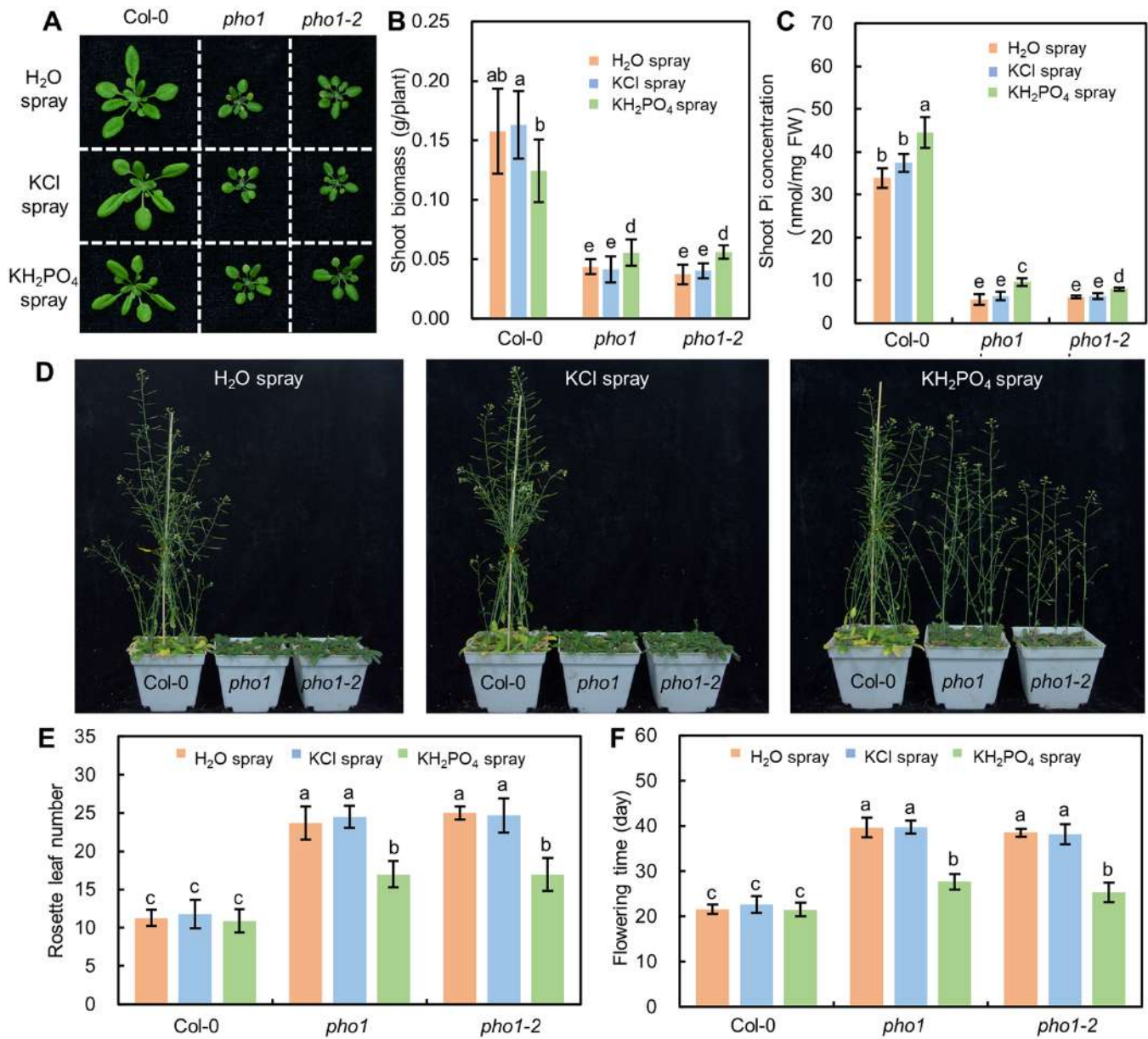


Fig. 2. Late flowering phenotype of *pho1* mutants can be partially recovered by Pi spray in shoots. (A) Shoot phenotypes of 25-day-old plants after sprays with H₂O, KCl (10 mM, pH 7.0), and KH₂PO₄ (10 mM, pH 7.0) for 15 d under LDs. Shoot biomass (B) and shoot available phosphate concentrations (C) in Col-0, *pho1*, and *pho1-2* plants sprayed with H₂O, KCl, and KH₂PO₄. (D) Phenotype of 44-day-old Col-0, *pho1*, and *pho1-2* plants after treatments with H₂O spray, KCl spray, and KH₂PO₄ spray under LDs. Flowering times were measured by counting rosette leaf number at bolting (E) and the days at bolting (F) ($n=16$, \pm SD). The shoots of plants were sprayed with the solution every 2 d. Different letters indicate that values are significantly different at $P<0.05$ (Student's *t*-test).

Modulating Pi signaling components upstream of PHO1 alters flowering time

We further investigated whether flowering is affected by the modulation of upstream signaling components of PHO1. The protein abundance of PHO1 is regulated through PHO2-dependent ubiquitination-mediated degradation, and knockout mutation of *PHO2* leads to the increase of PHO1 abundance and the accumulation of shoot Pi (T.Y. Liu et al., 2012). Here,

the RLN and the number of days at bolting were reduced in the *pho2* mutant, which showed an early flowering phenotype (Fig. 6A–C). However, the early flowering phenotype disappeared when *pho2* mutant plants were grown under low Pi conditions (Fig. 6D–F). Under low Pi conditions, the Pi concentration of *pho2* was similar to that of the WT (Supplementary Fig. S6). These results suggest that the early flowering of *pho2* is associated with Pi accumulation. The growth and the Pi concentration of the *pho1 pho2* double mutant were similar to those of

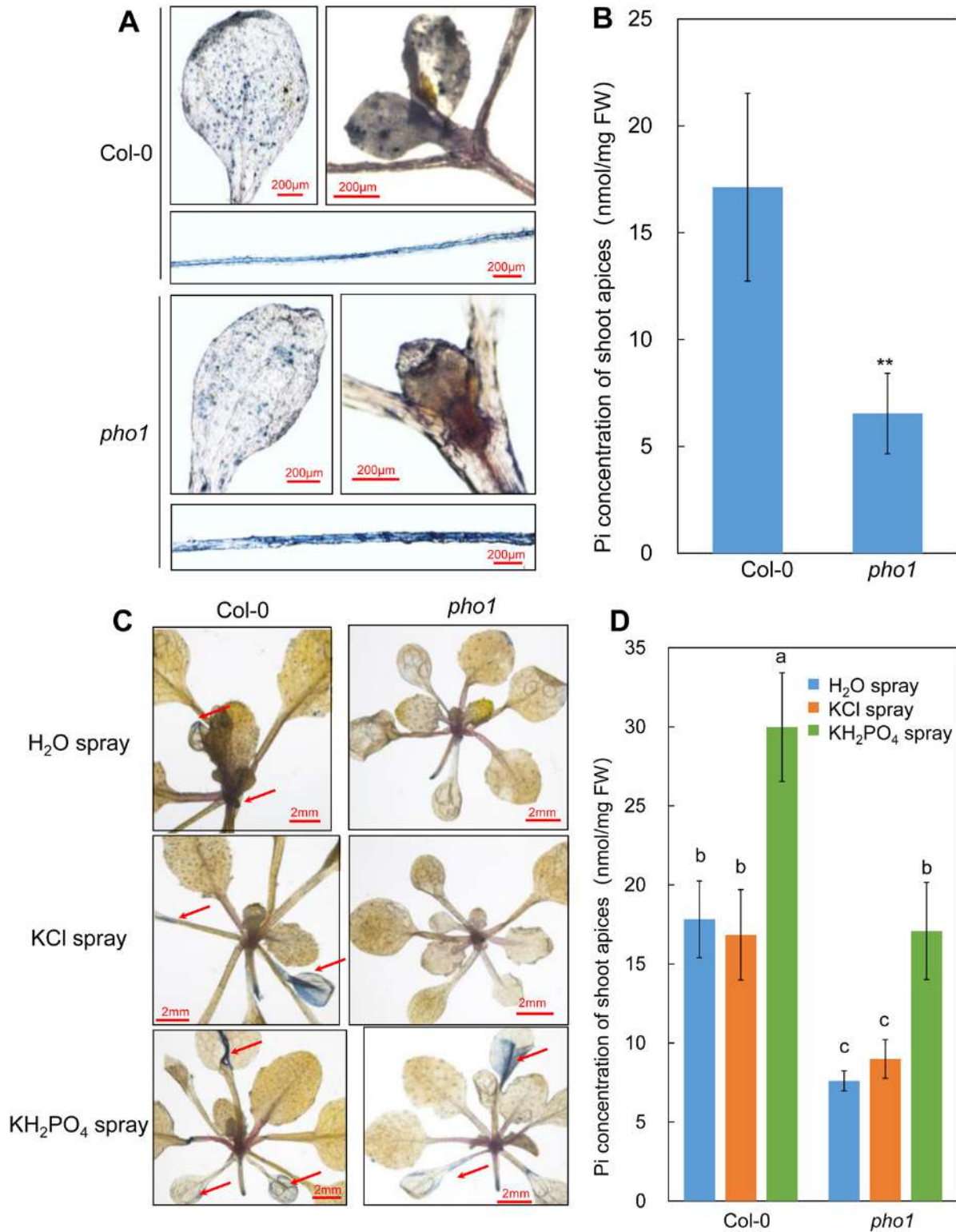


Fig. 3. Pi staining and Pi concentration in the shoot apices of Col-0 and *pho1* plants before and after Pi spray. (A) Pi staining of cotyledons, shoot apices, and roots of Col-0 and *pho1* seedlings (7 d old) grown in 1/2 MS medium with the IOSA method. (B) Pi concentration in the shoot apices of 20-day-old Col-0 and *pho1* mutant plants grown in soil under LD conditions. (C) Pi staining of shoot apices and leaves of Col-0 and *pho1* plants (20 d old) after spraying with H₂O, KCl, or KH₂PO₄ for 11 d with the IOSA method. Leaves with blue color after Pi staining are indicated by red arrows. (D) Pi concentration in the shoot apices of Col-0 and *pho1* mutant plants grown in soil after spraying with H₂O, KCl, or KH₂PO₄ for 11 d. For the IOSA Pi staining, blue intensity is positively correlated to the Pi concentration in the corresponding tissues. Shoot apices were harvested by removing the cotyledons and all leaves >5 mm. Two asterisks indicate a significant difference between Col-0 and *pho1* mutants by Student's *t*-test (***P*<0.01). Different letters indicate that values are significantly different at *P*<0.05 (Student's *t*-test).

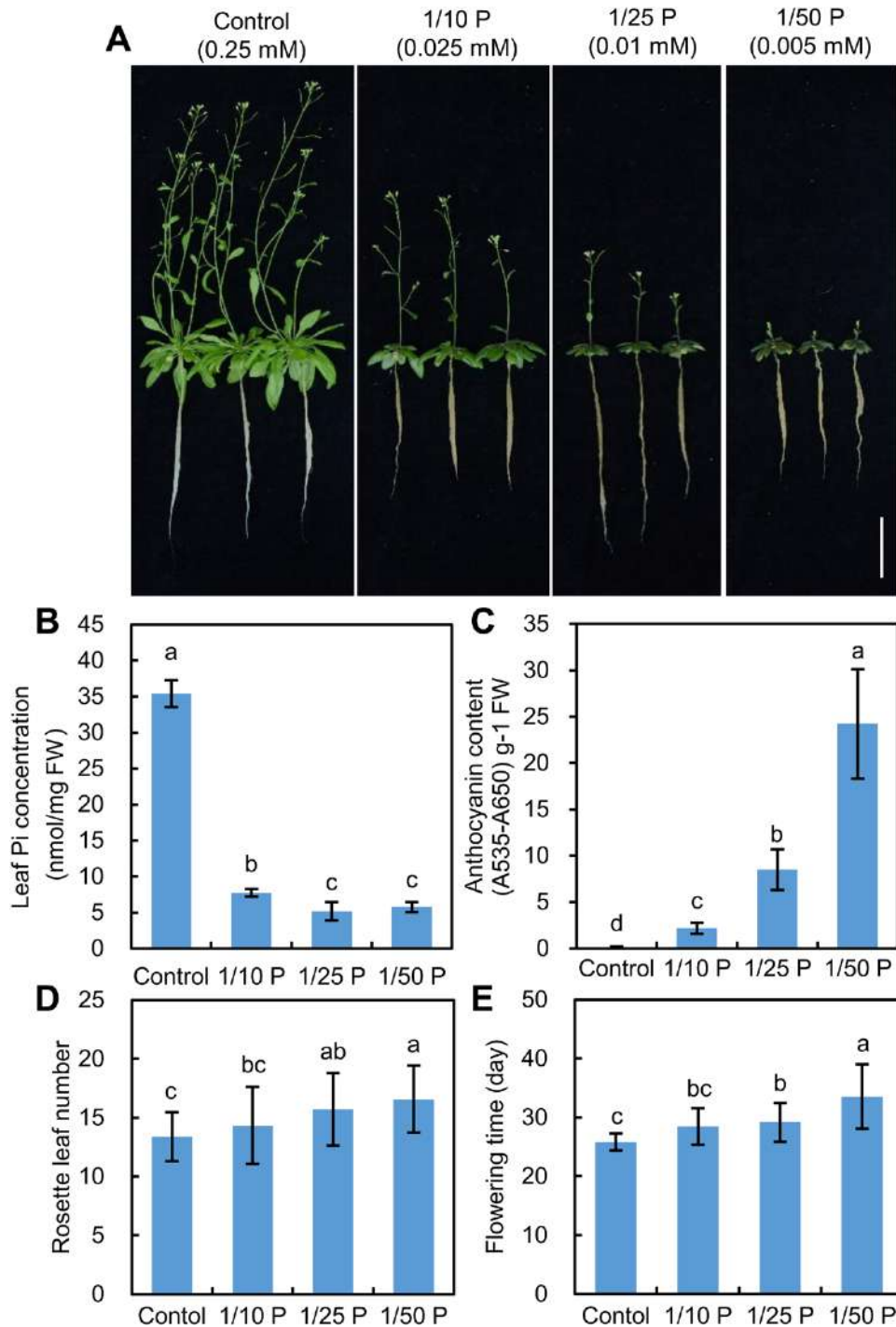


Fig. 4. Effect of Pi concentration in the hydroponic culture medium on the flowering time of wild-type plants (Col-0) under LDs. (A) Growth phenotypes of 39-day-old wild-type (Col-0) plants grown in hydroponic culture with different Pi concentrations under LD conditions. Scale bar, 5 cm. Leaf Pi concentration (B) and leaf anthocyanin content (C) were measured. Flowering times were measured by counting the rosette leaf number at bolting (D) and the days at bolting (E) in Col-0 plants under control and low phosphorus conditions ($n=16$, \pm SD). Different letters indicate that values are significantly different at $P<0.05$ (Student's t -test).

pho1 (Supplementary Fig. S6), and these two mutants showed late flowering phenotypes under both normal Pi and low Pi conditions (Fig. 6D–F). These results suggest that PHO1 is epistatic to PHO2 in flowering time regulation, and the early

flowering of *pho2* may result from the increase of PHO1-mediated Pi translocation.

We also analyzed the flowering time of *phr1* and *phl1* mutants. Although there was no significant difference in the

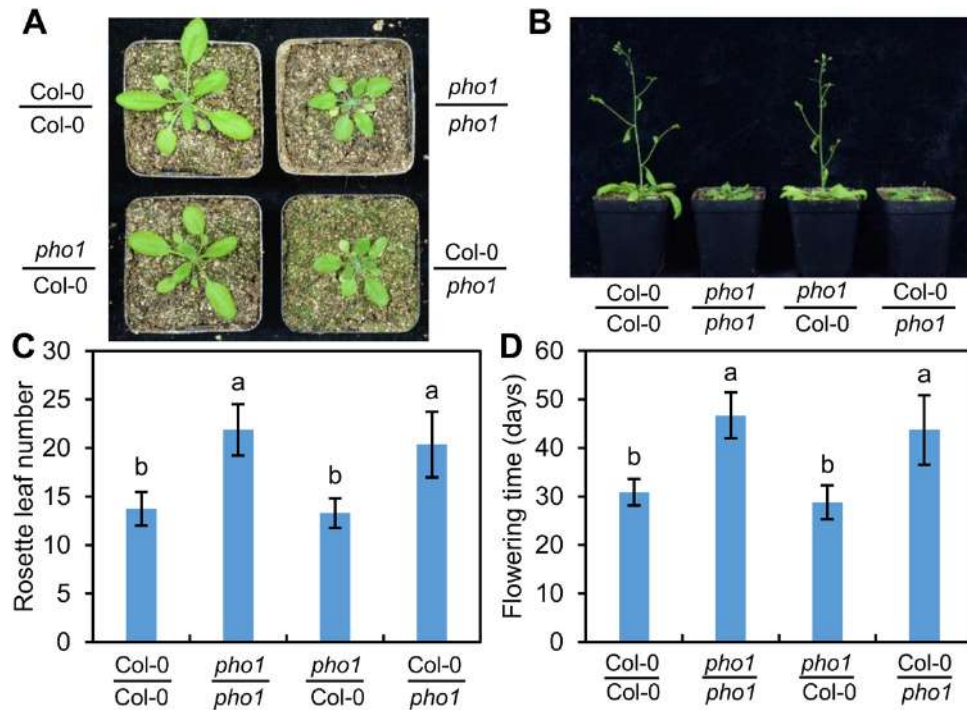


Fig. 5. Growth and flowering phenotypes in grafted plants of Col-0/Col-0, *pho1/pho1*, *pho1*/Col-0, and Col-0/*pho1*. (A) Grafted plants (33 d old) grown in soil under LD conditions. The photo was taken 20 d after transplanting to soil. (B) Flowering phenotypes of grafted plants (43 d old). Flowering times were measured by counting rosette leaf number at bolting (C) and the days at bolting (D) ($n=16$, \pm SD). Different letters indicate that values are significantly different at $P<0.05$ (Student's t -test).

RLN at bolting between *phr1* or *phl1* and the WT, the days at bolting were increased in *phr1* when compared with the WT (Supplementary Fig. S7A–C). In addition, both the RLN and the days at bolting were significantly higher in the *phr1 phl1* double mutant when compared with the WT (Supplementary Fig. S7A–C). These results suggest that PHR1 and PHL1 play a positive role in the floral transition, possibly by influencing the root-to-shoot translocation of Pi. We also tried to generate a *pho1 phr1* double mutant, but the growth of this double mutant is extremely weak and it is difficult to obtain its seeds. We also generated a *pho1 spx1 spx2* triple mutant to investigate the effect of SPX1/2 mutation or PHR1 enhancement on the late flowering of *pho1*. The growth, Pi concentration, and anthocyanin content of the *pho1* mutant were partially recovered by the knockout mutation of SPX1/2 (Supplementary Fig. S8). Although the mutation of SPX1/2 did not affect flowering time, the late flowering of *pho1* could be partially rescued by the mutation of SPX1/2 (Supplementary Fig. S7D–F).

Knockout mutation of *PHO1* alters the expression of flowering time genes

To investigate the molecular basis for the late flowering of *pho1* mutants, we analyzed the transcriptome of *pho1* shoots after spraying with KCl or KH_2PO_4 for 11 d by RNA-seq, and identified the DEGs. After excluding the low-quality reads,

41.5–52.4 million reliable clean reads were acquired from each library, and most of the clean reads (>97.4%) could be mapped to the Arabidopsis reference genome (Supplementary Table S2). The Pearson's correlation values (R) of three biological replicates of each sample were all >95% (Supplementary Table S3), indicating the high reliability of these replicates. The expression level of each transcript was calculated according to the TPM, and a total of 37 763 gene loci were detected among all these samples (Supplementary Tables S4, S5). By differential expression analyses (\log_2 fold change ≥ 1 or ≤ -1 , and adjusted P -value ≤ 0.05), a total of 990 DEGs were identified in *pho1* when compared with the WT under KCl spray (Fig. 7A, B; Supplementary Table S6). Among them, 559 DEGs were up-regulated, and 80 GO terms were significantly enriched (adjusted P -value ≤ 0.05), such as cellular response to starvation, and ion transport; 431 DEGs were down-regulated, and 33 GO terms were significantly enriched, such as response to hormone, and developmental process (Supplementary Fig. S9; Supplementary Table S7). Notably, under KH_2PO_4 spray, the number of DEGs in *pho1* was reduced to 448 compared with the WT (Fig. 7A, B; Supplementary Table S6). As shown in the Venn diagram, 742 DEGs (75%) in *pho1* under KCl spray compared with the WT were recovered by KH_2PO_4 spray (Fig. 7D); 38 GO terms were enriched (adjusted P -value ≤ 0.05) in these DEGs, such as flavonoid biosynthetic process and response to JA (Fig. 7E; Supplementary Table S7). These results

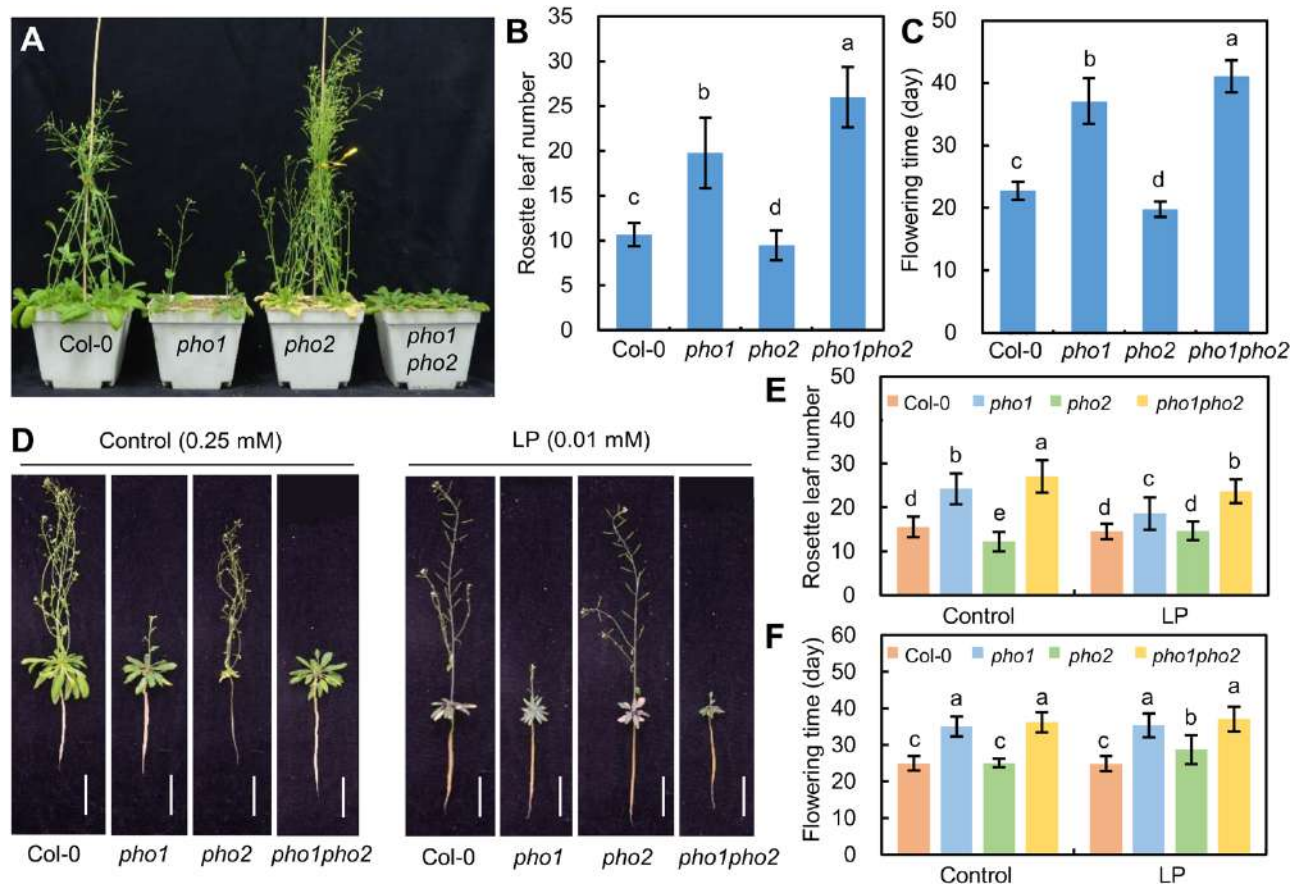


Fig. 6. Flowering phenotype of the *pho1pho2* double mutant. (A) Flowering phenotypes of 43-day-old Col-0, *pho1*, *pho2*, and *pho1pho2* plants growing in soil under LDs. The flowering times were measured by counting the rosette leaf number at bolting (B) and the days at bolting (C) in Col-0, *pho1*, *pho2*, and *pho1pho2* plants ($n=16$, \pm SD). (D) Phenotypes of 43-day-old Col-0, *pho1*, *pho2*, and *pho1pho2* plants grown under hydroponic culture with different Pi concentrations (control, 0.25 mM Pi; LP, 0.01 mM Pi). Flowering times were measured by counting the rosette leaf number at bolting (E) and the days at bolting (F) in Col-0, *pho1*, *pho2*, and *pho1pho2* plants under control and low phosphorus conditions ($n=16$, \pm SD). Different letters indicate that values are significantly different at $P<0.05$ (Student's *t*-test).

suggest that the expression of genes altered by *PHO1* knockout can be recovered by Pi supplementation in shoots. In addition, 59 DEGs were found to be commonly responsive to Pi spray in both *pho1* and WT plants when compared with KCl spray (Fig. 7F; Supplementary Table S6); 29 GO terms were enriched (adjusted P -value ≤ 0.05) for these DEGs, such as response to JA and defense response (Fig. 7G; Supplementary Table S7).

Through the transcriptomic analyses, at least 15 genes associated with flowering time regulation were identified to be differentially expressed in *pho1* under either KCl spray or KH_2PO_4 spray as compared with the WT (Fig. 8A). Among these genes, six genes encoding activators of floral transition, namely *TFS1*, *LFY*, *SPL4*, *FUL*, *SEP3*, and *AP1* (Kinoshita and Richter, 2020), were found to be down-regulated in *pho1* shoots under KCl spray, but were recovered by Pi spray when compared with the WT (Fig. 8A). In addition, four genes encoding repressors of floral transition, namely *SMZ*, *NFYA4*, *RGL2*, and *MYC4* that were induced in *pho1* shoots under

KCl spray, were found to be recovered by Pi spray (Fig. 8A). Therefore, knockout mutation of *PHO1* altered a group of flowering time-associated genes, and this was rescued by external Pi supplementation in shoots. The late flowering phenotype of *pho1* mutants may be caused by the repressed expression of genes encoding floral transition activators and/or by the increased expression of genes encoding floral transition repressors.

To investigate which flowering pathway is putatively implicated in *PHO1*-regulated flowering, we examined the diurnal expression patterns of several key flowering pathway integrators in *pho1* and WT seedlings by qRT-PCR. The expression of *FT* and *TSF*, the homolog of *FT*, two key regulators of the floral transition, was found to be dramatically reduced in *pho1* when compared with the WT at the time point of Zeitgeber time (ZT) 16 (Fig. 8B, C), whereas, the expression of other floral pathway integrator genes, such as *CO*, *SOC1*, *FLC*, and *SVP* (Kinoshita and Richter, 2020), was not significantly

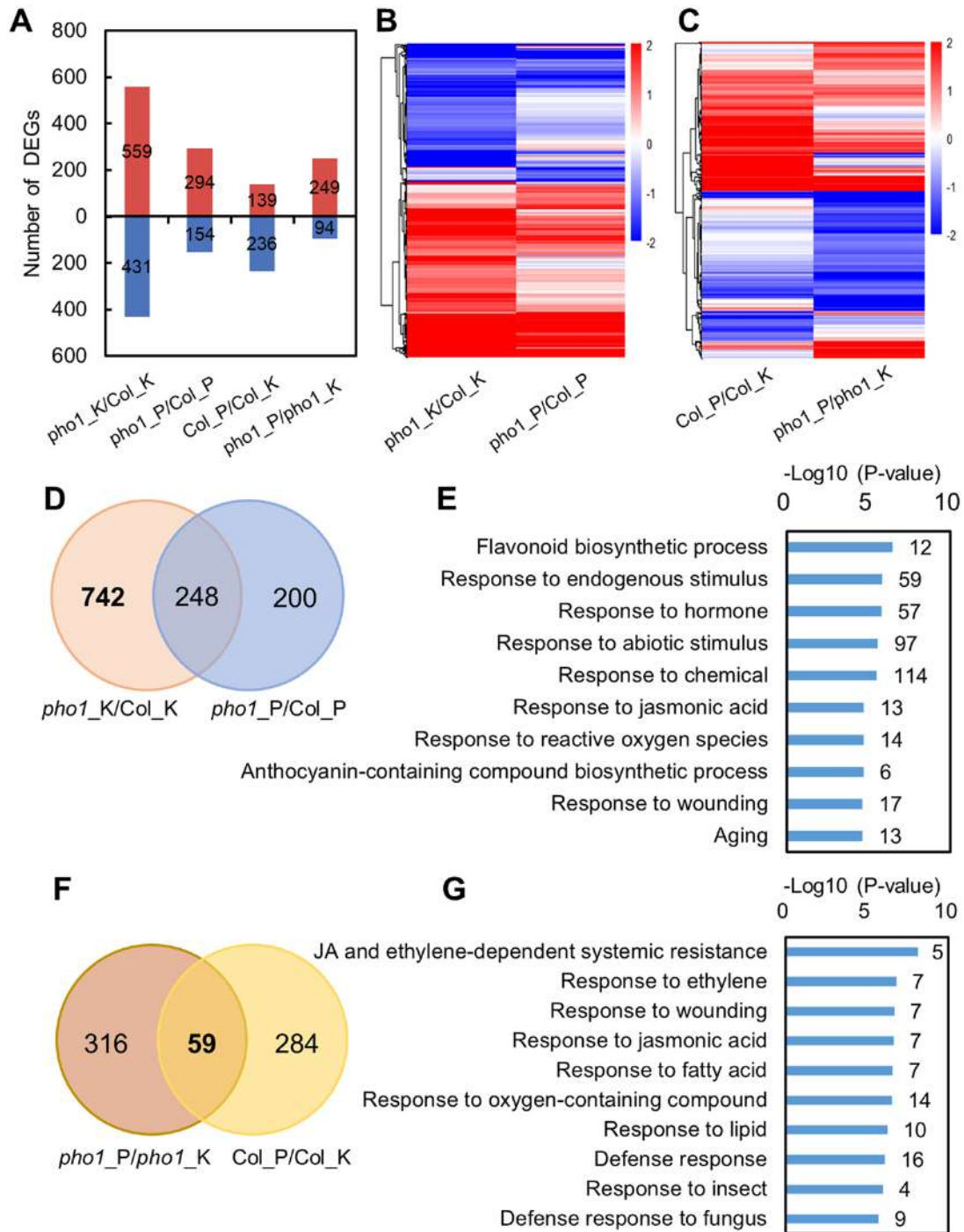


Fig. 7. Differentially expressed genes (DEGs) identified by transcriptome analyses and enriched GO terms of DEGs in *pho1* sprayed with KCl or KH_2PO_4 . (A) The numbers of up- and down-regulated DEGs in shoots of the *pho1* mutant under KCl spray (*pho1_K*) and KH_2PO_4 spray (*pho1_P*) for 11 d as compared with those in wild-type Col-0 (*Col_K* and *Col_P*). The whole rosettes of plants were collected at ZT10 and used for RNA-seq analysis. (B) Heat maps showing the expression patterns and clustering of DEGs in *pho1* compared with the WT under KCl and KH_2PO_4 spray. (C) Heat maps showing the expression patterns and clustering of DEGs in *pho1* and the wild type under KH_2PO_4 spray compared with KCl spray. Genes differentially expressed (\log_2 fold change ≥ 1 or ≤ -1 , adjusted P -value ≤ 0.05) under at least one of these comparisons were selected for analysis. \log_2 fold change was used for the hierarchical clustering analysis based on Euclidian distance. (D) Venn diagram representing the overlapping DEGs between *pho1* and the wild type under KCl and KH_2PO_4 sprays. (E) The 10 most enriched GO terms in the 742 DEGs in *pho1* under KCl spray but not under KH_2PO_4 spray. The number of genes belonging to the GO term is shown next to the bar. (F) Venn diagram representing the overlapping DEGs under Pi spray (KH_2PO_4 spray versus KCl spray) in both *pho1* and the wild type. (G) The 10 most enriched GO terms in the common 59 DEGs under Pi spray in both *pho1* and the wild type. The number of genes belonging to the GO term is shown next to the bar.

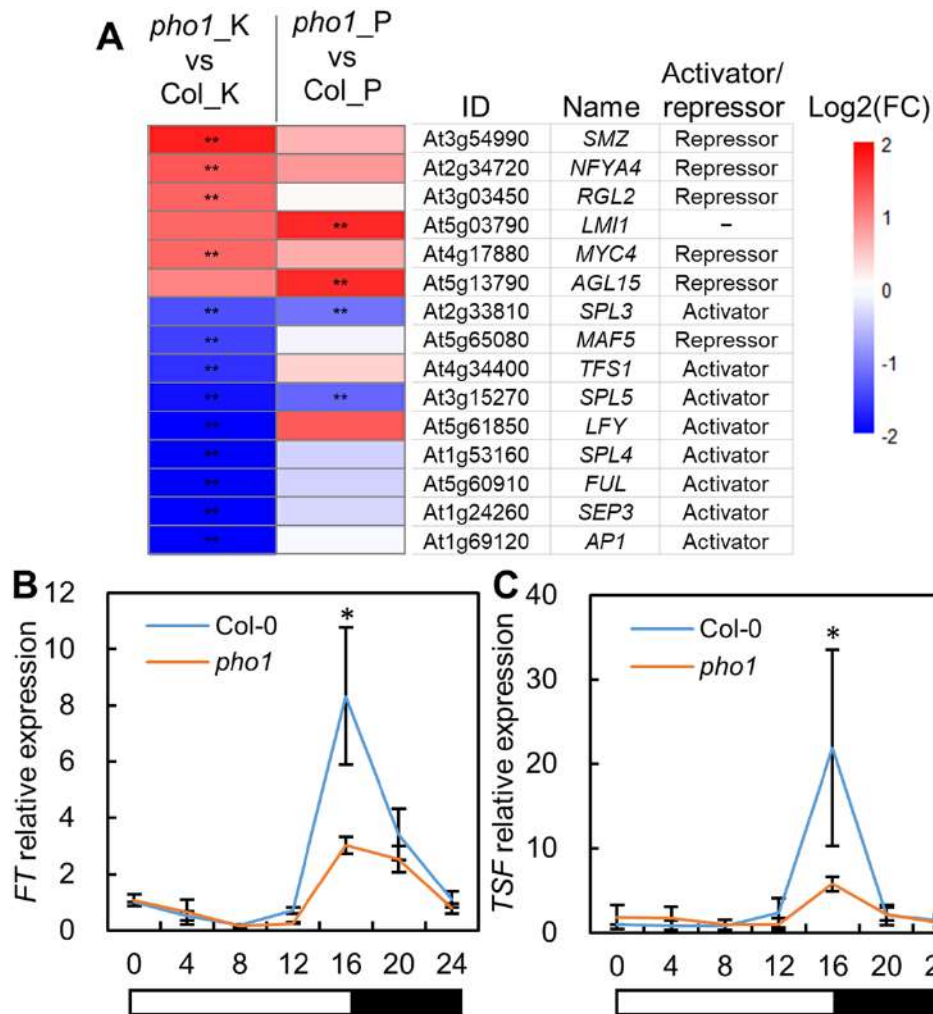


Fig. 8. Expression pattern of genes associated with flowering time regulation in *pho1*. (A) Expression of genes associated with flowering time regulation in *pho1* sprayed with KCl or KH_2PO_4 as revealed by RNA-seq. Two asterisks (**) indicate significant changes (an absolute fold change >2 and P -value <0.05). Diurnal expression profiles of *FT* (B) and *TSF* (C) in wild-type (Col-0) and *pho1* seedlings collected 9 d after germination grown under LD conditions over a 24 h period after dawn (ZT=0). The maximum expression value of each gene at a time point was normalized to 100%. Experiments were performed with three biological replicates ($n=3$, $\pm\text{SD}$). Asterisks (*) indicate significant differences (Student's t -test, $P<0.05$).

changed in *pho1* mutants (Supplementary Fig. S10). Therefore, the late flowering phenotype of the *pho1* mutant may be associated with the FT/TSF-mediated flowering pathway.

Genetic analyses of the interaction between PHO1 and flowering pathway integrators

We next examined the genetic interaction between PHO1 and FT by analyzing the effect of *FT* expression modulation on the flowering time of *pho1* mutants. We crossed different types of *FT* overexpression lines (L. Liu et al., 2012) and the knockout mutant *ft-10* (Xu et al., 2022) with *pho1*. Overexpression of *FT* in whole plants driven by the 35S promoter, or expression of *FT* in the shoot apical meristem (SAM) driven by the *KNAT1* promoter in the background of the *pho1* mutant, resulted in early flowering, which is similar to the corresponding

FT overexpression lines in the background of the WT (Fig. 9A–F). These results suggest that PHO1-regulated flowering is associated with FT. Given that *PHO1* is expressed in the vascular cylinder, which is similar to *FT*, we further investigated whether *PHO1* mutation affects the movement of FT. However, *PHO1* mutation did not affect the early flowering caused by overexpression of *FT* in the phloem companion cells driven by the *SUC2* promoter (Fig. 9G–I). Y2H assay indicated that there was no protein interaction between PHO1 and FT (Supplementary Fig. S11). In addition, genetic analysis showed that the double mutant *pho1 ft-10* flowered later than the individual *ft-10* or *pho1* mutants under LD or SD conditions (Supplementary Fig. S12). Thus, PHO1 could not affect the movement of FT protein to the SAM.

We then investigated the possible genetic interactions between PHO1 and other floral integrators including CO, FLC,

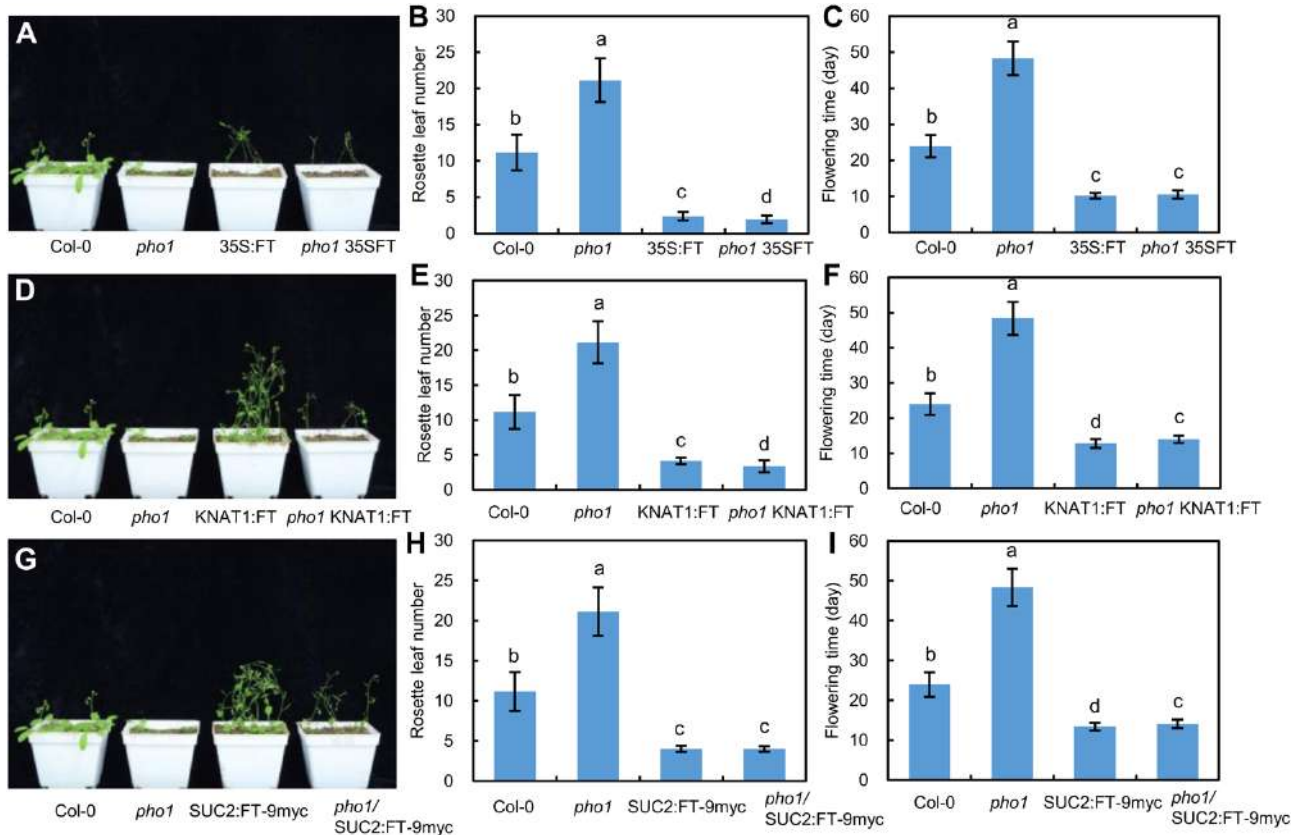


Fig. 9. Flowering phenotypes of *pho1* mutant plants and *FT* overexpression transgenic plants (*pho1* background) driven by different promoters. (A) Phenotypes of 36-day-old wild-type (Col-0), *pho1*, 35S:FT, and *pho1* 35S:FT plants grown in soil under LD conditions. Flowering times were measured by counting the rosette leaf number at bolting (B) and the days at bolting (C) in wild-type (Col-0), *pho1*, 35S:FT, and *pho1* 35S:FT plants under LD conditions ($n=16$, \pm SD). (D) Phenotypes of 31-day-old wild-type (Col-0), *pho1*, KNAT1:FT, and *pho1* KNAT1:FT plants grown in soils under LD conditions. Flowering times were measured by counting the rosette leaf number at bolting (E) and the days at bolting (F) in wild-type (Col-0), *pho1*, KNAT1:FT, and *pho1* KNAT1:FT plants under LD conditions ($n=16$, \pm SD). (G) Phenotypes of 36-day-old wild-type (Col-0), *pho1*, SUC2:FT-9myc, and *pho1* SUC2:FT-9myc plants grown in soil under LD conditions. Flowering times were measured by counting the rosette leaf number at bolting (H) and the days at bolting (I) in wild-type (Col-0), *pho1*, SUC2:FT-9myc, and *pho1* SUC2:FT-9myc plants under LD conditions ($n=16$, \pm SD). Different letters indicate that values are significantly different at $P<0.05$ (Student's *t*-test).

SOC1, and SVP. The RLN of *pho1 co-9* at bolting was similar to that of *co-9*, but was significantly higher than that of *pho1* under LDs (Supplementary Fig. S13A–C). The number of days at bolting of *pho1 co-9* was higher than that of *pho1* or *co-9* under LD conditions (Supplementary Fig. S13A–C). These results suggest the potential involvement of CO in PHO1-mediated flowering regulation under LD conditions. Under SD conditions, *pho1 co-9* showed a late flowering phenotype similar to that of *pho1* by scoring the number of days at bolting, but the RLN of *pho1* and *pho1 co-9* was less than that of the WT (Supplementary Fig. S13D–F), suggesting that the late flowering of *pho1* may be independent of CO under SD conditions.

Genetic interaction analyses showed that *pho1 flc-3* exhibited intermediate flowering time phenotype between *pho1* and *flc-3*; the RLN of *pho1 flc-3* at bolting and the number of days at bolting were between that of *pho1* and *flc-3*, though they were significantly higher than that of the WT (Supplementary

Fig. S14A–C). These results suggest a lack of genetic interaction between PHO1 and FLC in floral transition regulation (Supplementary Fig. S14A–C). In addition, the *pho1 soc1-2* double mutant showed a synergistic effect when compared with the *pho1* or *soc1-2* single mutant; the RLN and the number of days at bolting of *pho1 soc1-2* were dramatically higher than that of single mutants (Supplementary Fig. S14D–F), suggesting that PHO1 and SOC1 may act independently in the control of floral transition.

We also generated the *pho1 svp-41* double mutant and compared the flowering phenotype with that of *pho1 svp-41*, and the WT under different temperatures (23 °C and 16 °C). The flowering time of *Arabidopsis* was significantly delayed under 16 °C as compared with 23 °C, and the loss-of-function mutant *svp-41* showed less sensitivity to ambient temperature changes (Supplementary Fig. S15), which is consistent with previous reports (Lee *et al.*, 2007). Similar to *svp-41*, *pho1 svp-41* exhibited an early flowering phenotype insensitive to

ambient temperature changes (Supplementary Fig. S15). These results suggest that SVP may be required for the late flowering of *pho1* mutants.

Late flowering phenotype of *pho1* mutants is rescued by blocking the jasmonic acid signaling pathway

Given that loss of PHO1 leads to JA accumulation (Khan *et al.*, 2016), and that JA plays a negative role in floral transition (Zhao *et al.*, 2022), we hypothesized that the late flowering of *pho1* mutants may be associated with JA signaling. Here, through RNA-seq analysis, at least 13 genes that are responsive to JA were found to be differentially expressed in *pho1* under KCl spray and were recovered by Pi spray when compared with the WT (Supplementary Fig. S16). These genes included five genes that were up-regulated under KCl but were recovered by Pi spray in *pho1*, namely *MDHAR*, *PRB1*, *UF3GT*, *TT4*, and *CYT1*. Among these DEGs responsive to JA, 10 were also responsive to Pi spray in *pho1* or the WT as compared with KCl spray, including six genes (*COR13*, γ -*VPE*, *TPS03*, *PDF1.2*, *PDF1.2b*, and *PDF1.2c*) that were down-regulated by KCl spray but were up-regulated by Pi spray in *pho1* (Supplementary Fig. S16). These results suggest that the JA response is influenced by the loss of *PHO1*, and is also affected by external Pi supplementation in shoots.

CORONATINE INSENSITIVE 1 (*COI1*) is an F-box protein that functions as an essential component of the JA perception machinery by recruiting a functional E3 ubiquitin ligase SCF^{COI1} to target the jasmonate-ZIM domain (JAZ) proteins (Wasternack and Song, 2017). Therefore, we generated the *pho1 coi1-2* double mutant by crossing *pho1* with *coi1-2*, which harbors a point mutation of *COI1* (Zhai *et al.*, 2015), to test whether the late flowering of *pho1* mutants is associated with JA signaling. The shoot FW of the double mutant *pho1 coi1-2* was significantly higher than that of *pho1*, but it was still lower than that of the WT (Fig. 10A, B). The shoot Pi concentration of *pho1 coi1-2* was similar to that of the *pho1* parent and was much lower compared with the WT (Fig. 10C). The anthocyanin level in rosettes of *pho1 coi1-2* was similar to that of *coi1-2*, and was much lower than that of *pho1*, which accumulated anthocyanin in rosettes, a phenotype typically associated with Pi deficiency (Supplementary Fig. S17A, B). In addition, we compared the growth phenotypes of *pho1*, *coi1-2*, and *pho1 coi1-2* mutant seedlings upon methyl jasmonate (MeJA) treatment on medium with or without Pi. The FW and root length of WT and *pho1* seedlings were significantly repressed by the presence of 20 μ M MeJA under Pi-sufficient conditions, where the growth of *coi1-2* and *pho1 coi1-2* seedlings was insensitive to MeJA treatment (Supplementary Fig. S17C–E). These results suggest that JA signaling is impaired in *pho1 coi1-2*, which is similar to what occurs in *coi1-2*. By measuring the RLN and days at bolting, the late flowering phenotype of *pho1* was partially rescued by the mutation of *COI1* (Fig. 10D–F). Consistently, the expression of *FT* in *pho1 coi1-2*

was significantly increased compared with that in *pho1*, but it was still lower than that of the WT (Fig. 10G).

Conjugated JA-Ile is the bioactive form of JA, and its biosynthesis is catalyzed by the enzyme encoded by the JA-resistance 1 (*JAR1*) gene (Staswick and Tirryaki, 2004). We also generated the *pho1 jar1-1* double mutant by crossing *pho1* with *jar1-1*, which harbors a point mutation of *JAR1* (Huang *et al.*, 2021), to assess the contribution of the JA signaling pathway in the late flowering of *pho1* mutants. The impaired growth and late flowering phenotypes of *pho1* mutants could at least be partially recovered by the knockout mutation of *JAR1*, although the shoot Pi concentration could not be rescued by *JAR1* mutation (Supplementary Fig. S18). Taken together, these results indicate that the induction of the JA signaling pathway is responsible for the late flowering phenotype of *pho1* mutants.

Mutation of *OsPHO1;2*, the homolog of *PHO1*, delays flowering in rice

To investigate whether the role of *PHO1* in floral transition is conserved in plant species, we generated the loss-of-function mutant of *OsPHO1;2*, the closest *PHO1* homolog in rice (Secco *et al.*, 2010), by CRISPR/Cas9-mediated gene editing for phenotype analysis. One homozygous line named *Ospho1;2-crispr* was acquired with a deletion of 48 bp in the third exon of *OsPHO1;2* (Fig. 11A). The shoot length, root length, and FW of the *Ospho1;2-crispr* mutant were significantly lower than those of WT seedlings (Fig. 11B–E). Notably, the shoot Pi concentration of the *Ospho1;2-crispr* mutant were dramatically lower than that of the WT, whereas the root Pi concentration of the *Ospho1;2-crispr* mutant was higher than that of the WT (Fig. 11F), suggesting the impairment of Pi translocation from roots to shoots by *OsPHO1;2* knockout. The *Ospho1;2-crispr* mutant showed a delayed flowering phenotype compared with the WT (Fig. 11G). The days from sowing to heading for *Ospho1;2-crispr* were significantly greater than in the WT (Fig. 11H). We also measured the expression of *Hd3a* and *RFT1*, the homologs of *FT* in rice seedlings (Vicentini *et al.*, 2023), and found that these two genes were both significantly repressed in the *Ospho1;2-CRISPR* mutant (Fig. 11I). Therefore, the loss of *OsPHO1;2* homologous to *PHO1* also delays floral transition in rice by down-regulating the expression of *Hd3a* and *RFT1*.

Discussion

External Pi levels have been demonstrated for a long time to influence plant flowering timing (Menary and Staden, 1976; Rossiter, 1978), but the underlying molecular mechanism is still unclear. *PHO1* has been known for decades to mediate Pi translocation from roots to shoots (Poirier *et al.*, 1991; Wege *et al.*, 2016), but whether and how it regulates floral transition is still unknown. In this study, we demonstrate that *PHO1*

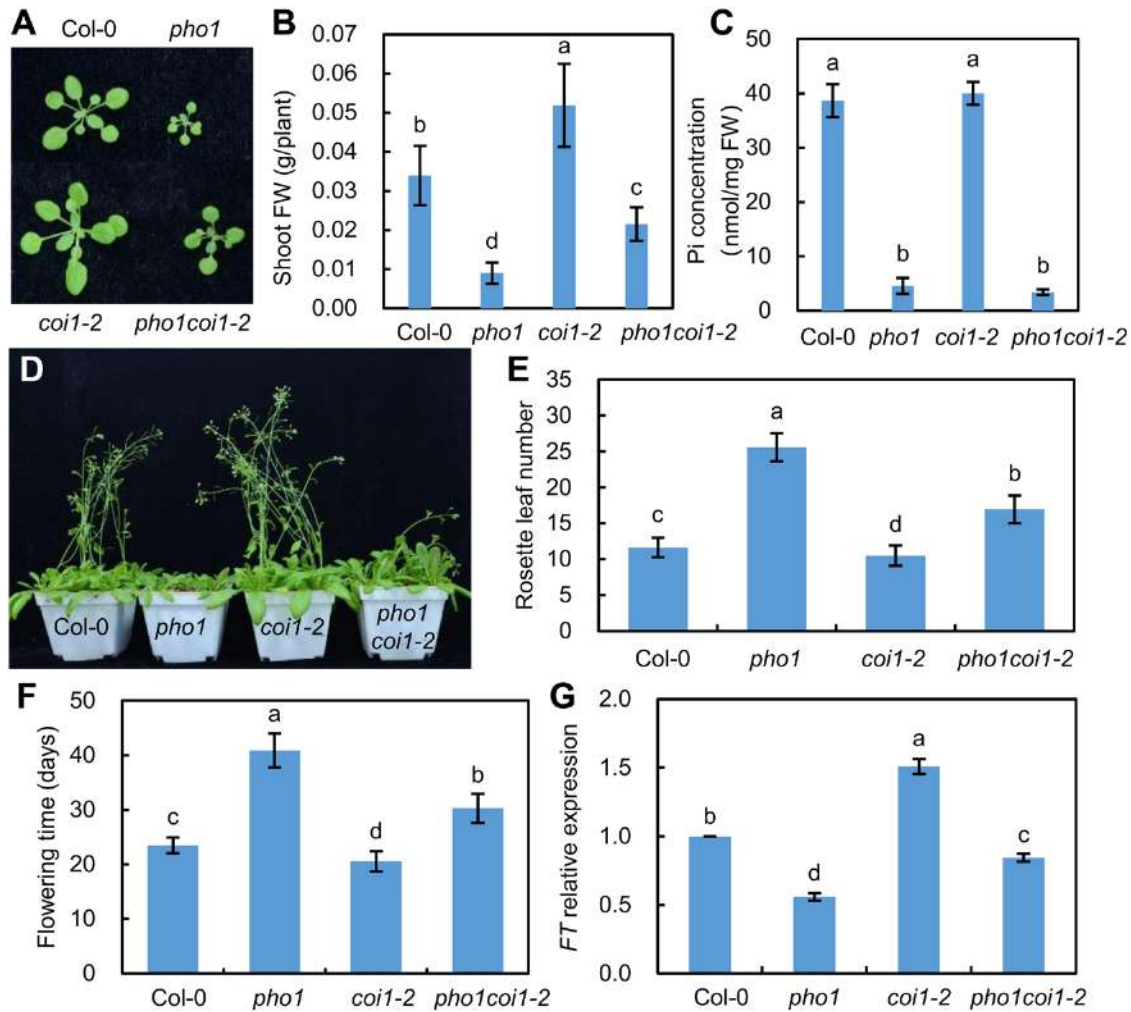


Fig. 10. Late flowering of *pho1* mutants is associated with JA signaling. (A) Phenotype of 19-day-old Col-0, *pho1*, *coi1-2*, and *pho1coi1-2* seedlings grown in soil. (B) Shoot FW of Col-0, *pho1*, *coi1-2*, and *pho1coi1-2* seedlings. (C) Shoot Pi concentration of Col-0, *pho1*, *coi1-2*, and *pho1coi1-2* seedlings. (D) Flowering phenotypes of 43-day-old wild-type (Col-0), *pho1*, *coi1-2*, and *pho1coi1-2* plants grown under LDs. Flowering times were measured by counting the rosette leaf number at bolting (E) and the days at bolting (F) under LDs ($n=16$, \pm SD). (G) Relative expression level of *FT* in Col-0, *pho1*, *coi1-2*, and *pho1coi1-2* seedlings. Samples used for qRT-PCR analysis were collected at ZT16. Different letters indicate that values are significantly different at $P<0.05$ (Student's *t*-test).

plays a positive role in flowering time regulation by mediating Pi translocation from roots to shoots in both Arabidopsis and rice. Loss of *PHO1* leads to late flowering by repressing the expression of *FT* and *TSF* in a JA-dependent manner. This work suggests that *PHO1* integrates P nutrition and flowering time in plants.

Arabidopsis *PHO1* has been known to be predominantly expressed in root stelar cells and plays a dominant role in root-to-shoot translocation of Pi by loading Pi into the xylem of roots (Hamburger *et al.*, 2002; Rouached *et al.*, 2011). Here, we show that the late flowering phenotype of *pho1* mutants resulted from impaired root-to-shoot Pi translocation based on several pieces of evidence. First, the late flowering of *pho1* mutants is not dependent on the Pi concentration in the growth medium, but it can be partially recovered by external Pi

spray or Pi application at the shoots (Fig. 2; Supplementary Fig. S3). Second, grafting experiments demonstrate that *PHO1*-mediated Pi translocation from roots to shoots is required for the proper floral transition (Fig. 5). Third, the flowering time of the WT is delayed by extremely low Pi in the growth conditions (Fig. 4). Therefore, Pi translocation from roots to shoots regulates the floral transition in plants.

In this study, we found that the late flowering of *pho1* mutants can be partially rescued by Pi application at shoot apices, where flowers initiate (Supplementary Fig. S4). The Pi concentration in the shoot apices of *pho1* mutants was found to be significantly lower than that of the WT, but it can be rescued by Pi spraying in the rosette (Fig. 3). Given that Pi is required for the biosynthesis of cellular components, such as ATP, nucleic acids, and membrane phospholipids (Dissanayaka *et al.*, 2021), a large

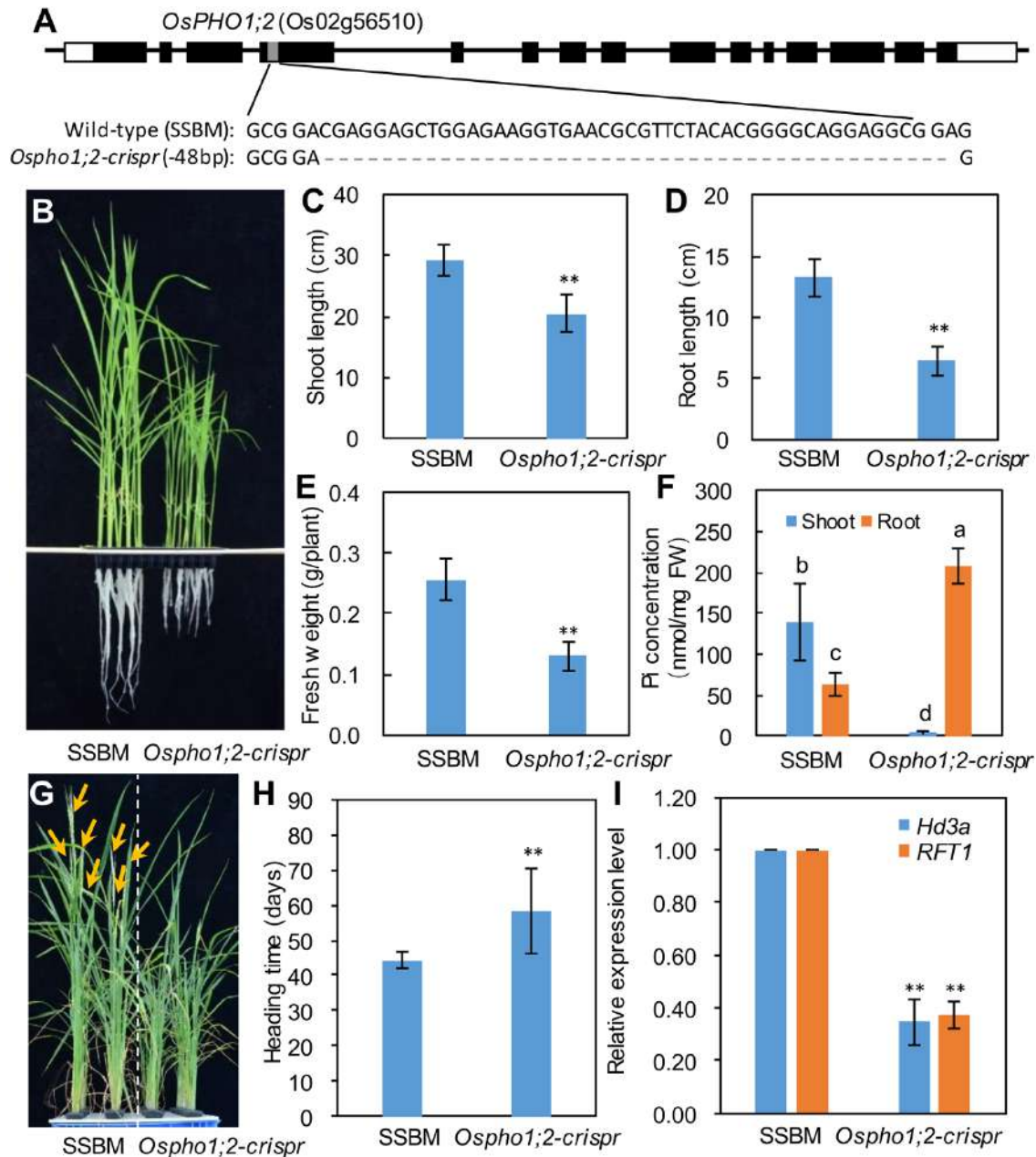


Fig. 11. Flowering phenotypes of the *Ospho1;2* mutant. (A) Gene structure and the CRISPR/Cas9-mediated mutation site of *OsPHO1;2*. The *Ospho1;2-crispr* mutant was generated by using a CRISPR/Cas9 genome-editing approach. (B) Morphological appearance of SSBM (wild-type) and *Ospho1;2-crispr* rice seedlings grown with hydroponic culture for 2 weeks under a 10 h/14 h photoperiod. Shoot length (C), root length (D), whole-plant FW (E), and Pi concentration (F) of 2-week old SSBM and *Ospho1;2-crispr* rice seedlings. (G) Flowering phenotypes of SSBM (wild-type) and the *Ospho1;2-crispr* mutant under SD (10/14 h) conditions. Arrows indicate panicles. (H) Days to heading of *Ospho1;2-crispr* mutant plants under SDs ($n=20$, \pm SD). (I) Relative expression level of *Hd3a* and *RFT1* in SSBM and the *Ospho1;2-crispr* mutant. Samples used for qRT-PCR analysis were collected at ZT4. Different letters indicate that values are significantly different at $P<0.05$ (Student's t -test). Two asterisks (**) indicate significant difference at $P<0.01$ (Student's t -test).

amount of Pi should be required in shoot apices for the development of leaves and floral organs. Therefore, Pi allocation into the SAM possibly contributed by PHO1 could be essential for proper floral transition. Similarly, nitrate has been suggested to function as a signal regulating flowering at the SAM

in Arabidopsis (Olas et al., 2019). It is possible that Pi may also act as a nutrient signal regulating floral transition at the SAM, which deserves further investigation. In addition, the leaf initiation rate was reduced by the knockout mutation of PHO1 (Supplementary Fig. S2). It is possible that sufficient Pi supply

is required for leaf initiation in the SAM, but the underlying mechanism deserves further investigation.

The protein abundance of PHO1 is negatively regulated by PHO2 through ubiquitination-mediated degradation, and knockout mutation of *PHO2* results in the increase of PHO1 and the accumulation of shoot Pi (T.Y. Liu *et al.*, 2012). Here, we found that knockout mutation of *PHO2* leads to early flowering under LD conditions, which is consistent with previous reports (Kim *et al.*, 2011). *PHO2* is negatively regulated by miR399, a small RNA that is up-regulated by Pi deficiency under the regulation of PHR1 and its homolog PHL1 (Aung *et al.*, 2006; Bari *et al.*, 2006). Transgenic Arabidopsis plants overexpressing miR399b also exhibit Pi overaccumulation in shoots and early flowering phenotypes (Kim *et al.*, 2011). Conversely, *phr1 phl1* double mutant plants which accumulate less Pi in shoots exhibit late flowering (Supplementary Fig. S7). Therefore, the early flowering phenotypes of *pho2* mutant and miR399-overexpressing plants could be associated with Pi overaccumulation in shoots. However, although the *spx1 spx2* double mutant accumulates Pi in shoots, its flowering time was not affected (Supplementary Figs S7, S8). It is possible that the Pi accumulation in shoots has to exceed a threshold value to trigger the Pi toxicity phenotype and early flowering.

Rice *PHO2* has been known to target *PHO1.2* for degradation (Wang *et al.*, 2020), and knockout mutation of *PHO2* results in Pi overaccumulation in shoots due to the increased Pi uptake and translocation (Hu *et al.*, 2011). Similar to the *pho1* mutants in Arabidopsis, knockout mutation of *PHO1.2* also results in late floral transition in rice (Fig. 11), suggesting that PHO1-mediated flowering regulation could be conserved in higher plants. Knockout mutation of *PHO2* results in early flowering in Arabidopsis (Kim *et al.*, 2011) (Fig. 6). However, the flowering time of the rice *pho2* mutant was delayed (Li *et al.*, 2017). Therefore, the role of rice *PHO2* in flowering time regulation should be different from that of Arabidopsis *PHO2*. It is interesting that rice *PHO2* interacts with *GI*, a key component in the photoperiodic flowering pathway, and the late flowering and Pi overaccumulation phenotypes are similar in both the *pho2* and *gi* mutants in rice (Li *et al.*, 2017). It is possible that rice *PHO2* plays a positive role in flowering regulation by interacting with *GI* and promoting photoperiod-mediated flowering, although it could also play a minor role in other flowering pathway by negatively regulating the abundance of *PHO1.2* and shoot Pi concentration. At present, it is still unclear whether *PHO2* interacts with *GI* in Arabidopsis. Whether the interaction between *PHO2* and *GI* happens specifically in plants such as rice and other cereals but not in plants such as Arabidopsis deserves further studies.

Transcriptomic analysis indicates that the knockout mutation of *PHO1* alters a group of genes associated with flowering time, and most of them could be recovered by applying exogenous Pi onto the rosettes (Fig. 8A). Among these genes, floral meristem identity genes *AP1*, *LFY*, and *FUL*, which are activated by upstream integrators such as *FT* and *SOC1* (Abe

et al., 2005; Li *et al.*, 2019), were repressed by *PHO1* mutation but were recovered by external Pi application. *SPL3/4/5*, which are targeted by miR156 and act synergistically with the FT-FD module to induce flowering by promoting the expression of *AP1*, *LFY*, and *FUL* (Jung *et al.*, 2016), were down-regulated by the loss of *PHO1*. Although *FT* was not differentially expressed in *pho1* mutants in the transcriptome analysis sampled at the time point of ZT10, qRT-PCR analysis indicated that the expression of *FT* and its homolog *TSF* is significantly reduced in *pho1* at ZT16 when compared with the WT (Fig. 8B, C). Therefore, *FT* could be the dominant floral integrator linked with the late flowering of *pho1* mutants. Genetic analyses by using a knockout mutant of *FT* and constitutive/tissue-specific *FT* overexpression lines also suggest that PHO1-mediated flowering regulation is associated with *FT*. However, based on the findings that PHO1 and *FT* do not interact with each other (Supplementary Fig. S11), that the flowering of the *pho1* scion is similar to that of WT scion when WT is used as the rootstock (Fig. 5), and that *PHO1* mutation does not affect the flowering time of vascular-specific *FT* overexpression lines (Fig. 9G–I), it is unambiguous that *PHO1* mutation could not affect the movement of *FT*.

The transcriptomic analysis suggests that the JA response is influenced by the loss of *PHO1*, which is consistent with previous findings that the loss of *PHO1* leads to JA accumulation (Khan *et al.*, 2016). In *pho1* mutants, the enhanced JA biosynthesis and subsequent JA-Ile formation by shoot Pi starvation is associated with stunted plant growth and increased anthocyanin accumulation in rosettes, as well as enhanced resistance to the herbivore *Spodoptera littoralis* (Khan *et al.*, 2016). The levels of 12-oxo-phytodienoic acid (OPDA), which is the JA precursor, JA, and JA-Ile have also been found to be increased by severe Pi deficiency in Arabidopsis (Simancas and Munné-Bosch, 2015). Transcriptomic studies also reveal changes in the expression of JA-related genes under Pi deficiency in plant species such as Arabidopsis, soybean, common bean, and white lupin (Morcuende *et al.*, 2007; Aparicio-Fabre *et al.*, 2013; Wang *et al.*, 2014; Zeng *et al.*, 2016). Recently, the molecular link connecting Pi starvation signaling and the JA signaling pathway has been revealed. Arabidopsis PHR1 is involved in JA signaling by interacting with JAZs and MYC2 and cooperatively modulating the transcription of downstream JA-responsive genes (He *et al.*, 2023). In rice, OsPHR2, the rice homolog of AtPHR1, binds to the promoter of *OsMYC2*, encoding a key transcription factor in JA signaling, and thus activates the expression of *OsMYC2* and modulates *OsMYC2*-mediated resistance to bacterial blight during Pi starvation (Kong *et al.*, 2021). *OsJAZ11*, a transcriptional repressor of JA signaling, is responsive to low Pi under the control of OsPHR2 and regulates Pi homeostasis by interacting with OsSPX1 (Pandey *et al.*, 2021).

It has been known that JA plays a negative role in floral transition (Song *et al.*, 2013; Wang *et al.*, 2017; Zhao *et al.*, 2022). The CO11-dependent JA signaling pathway delays

floral transition in *Arabidopsis thaliana* through the degradation of JAZ repressors and the further liberation of the transcriptional function of AP2 transcription factors, TOE1/2, to repress the expression of *FT* (Zhai *et al.*, 2015). Here, functional mutations of the JA receptor COI1, an F-box protein that targets JAZ proteins by recruiting the functional E3 ubiquitin ligase SCF^{COI1} (Wasternack and Song, 2017), as well as the mutation of JAR1 that catalyzes the biosynthesis of the bioactive form JA-Ile in the JA signaling pathway (Staswick and Tiriyaki, 2004), could partially rescue the growth inhibition and late flowering phenotypes of *pho1* mutants (Fig. 10; Supplementary Fig. S18). Therefore, the COI1-dependent JA signaling pathway is at least partially responsible for the late flowering phenotype of *pho1* mutants. In addition, transcriptomic analysis also revealed that the GO functional categories response to JA and JA/ethylene-dependent systemic resistance were significantly enriched in the common DEGs of *pho1* and the WT under external Pi spray (Fig. 7F, G). At least five JA-responsive genes were significantly induced by Pi spray as compared with KCl spray in both *pho1* and the WT (Supplementary Fig. S16), including the AP2/ERF domain transcription factor gene *ORA59* and its downstream gene *PDF1.2* that are induced by JA (Zarei *et al.*, 2011). Thus, it is possible that JA signaling is promoted under the external Pi spray. This seems contradictory to the induction of JA biosynthesis and signaling under Pi deficiency, and further studies are required to investigate the underlying molecular mechanisms.

Although there are no significant changes in the expression levels of floral integrator genes, such as *CO*, *SOC1*, *FLC*, and *SVP* (Richter *et al.*, 2019; Kinoshita and Richter, 2020), in *pho1* mutants (Supplementary Fig. S10), genetic analyses suggested that *CO* and *SVP* are potentially involved in PHO1-mediated flowering regulation under LD conditions (Supplementary Fig. S13, S14). *CO*, which is increased gradually during the daytime, plays a major regulatory role in the photoperiod flowering pathway by activating the expression of *FT* and *SOC1* under LDs (Suárez-López *et al.*, 2001; Valverde *et al.*, 2004). *CO* protein is stabilized under LDs but is degraded under SDs (Valverde *et al.*, 2004). Here, the knockout of *CO* further delayed the flowering time of *pho1* mutants under LDs, but had no effect under SDs (Supplementary Fig. S13), suggesting that the PHO1-mediated flowering regulation is putatively linked to the photoperiod pathway. *SVP* is a floral suppressor acting in ambient temperature-responsive flowering by inhibiting the expression of *FT* (Lee *et al.*, 2007). The *pho1 svp-41* double mutant showed an ambient temperature-insensitive early flowering phenotype, which was similar to that of the knockout mutant *svp-41* (Supplementary Fig. S15), suggesting that *svp* mutation is epistatic to *pho1*. Therefore, besides the JA signaling pathway, PHO1-mediated flowering may be associated with other flowering pathways, such as photoperiod and temperature pathways.

The functional knockout of *PHO1;2*, the rice homolog of *PHO1*, also delays floral transition in rice, which possibly

resulted from the down-regulation of *Hd3a* and *RFT1*, two homologs of Arabidopsis *FT* (Fig. 11). Because the homologs of *PHO1* are present in various flowering plants, and are involved in Pi translocation from roots to shoots (Secco *et al.*, 2010; He *et al.*, 2013; Zhao *et al.*, 2019; Nguyen *et al.*, 2021), it is possible that the PHO1-mediated flowering time regulation is conserved in higher plants including LD plants (such as Arabidopsis), SD plants (such as rice and soybean), and day-neutral plants (such as tomato). Because *PHO1* plays a dominant role in Pi translocation and Pi homeostasis, our work suggests that *PHO1* functions in the integration between Pi nutrition and flowering time regulation. In the future, a possible strategy to simultaneously regulate flowering time and P utilization efficiency may be realized by modulating the expression level of *PHO1* homologs in crop plants.

Supplementary data

The following supplementary data are available at *JXB* online.

Fig. S1. Diagrams of T-DNA insertion or point mutation mutants used in this study.

Fig. S2. Appearance of visible leaves (~2 mm in width) in the wild type (Col-0) and *pho1* and *pho1-2* mutants.

Fig. S3. Late flowering phenotype of *pho1* mutants is not dependent on external Pi concentration.

Fig. S4. Pi dip at leaves or shoot apices (SAs) partially rescued the late flowering phenotypes of *pho1* mutants.

Fig. S5. Representative GUS staining of *ProPHO1:GUS* transgenic seedlings.

Fig. S6. Growth phenotypes and leaf Pi concentration of 4-week-old Col-0, *pho1*, *pho2*, and *pho1pho2* plants grown under hydroponic culture with different Pi concentrations.

Fig. S7. Flowering phenotype of the *phr1phil1* double mutant and *pho1spx1spx2* triple mutant.

Fig. S8. Growth phenotypes, leaf Pi concentration, and anthocyanin content of 4-week-old Col-0, *pho1*, *spx1spx2*, and *pho1spx1spx2* seedlings grown in the soil.

Fig. S9. Expression patterns and GO enrichment of the up- or down-regulated genes in *pho1*.

Fig. S10. Diurnal expression of floral pathway integrator genes in *pho1* mutants.

Fig. S11. Yeast two-hybrid analysis of protein-protein interactions between *PHO1* and *FT*.

Fig. S12. Flowering phenotypes of the *pho1ft-10* double mutant.

Fig. S13. Effect of *CO* mutation on flowering of the *pho1* mutant.

Fig. S14. Effects of *FLC* mutation and *SOC1* mutation on the late flowering phenotypes of *pho1* mutants are partially rescued by *FLC* mutation, and are exacerbated by *SOC1* mutation.

Fig. S15. Effect of *SVP* mutation on the flowering phenotype of *pho1* mutant plants under LDs at 22 °C and 16 °C.

Fig. S16. Expression patterns of genes associated with JA metabolism and signaling that are differentially expressed in *pho1* under KCl spray or Pi spray or differentially expressed under Pi spray when compared with KCl spray.

Fig. S17. Phenotype of Col-0, *pho1*, *coi1-2*, and *pho1coi1-2* in response to treatments with low P and MeJA.

Fig. S18. Late flowering of *pho1* mutants can be restored by *JAR1* mutation.

Table S1. Primers used for genotyping and qRT-PCR analysis.

Table S2. Summary of the reads from RNA sequencing in all 12 libraries.

Table S3. Correlation (*R* value) of three biological replicates for RNA sequencing in shoots of Col and *pho1*.

Table S4. The expression levels (TPM value) of all genes in shoots of Col and *pho1*.

Table S5. RNA-seq analysis showing the expression of each locus in Col and *pho1* under Pi and KCl sprays.

Table S6. Differentially expressed genes in response to Pi spray or *PHO1* mutation.

Table S7. GO enrichment of differentially expressed genes.

Acknowledgements

We thank Drs Hao Yu (National University of Singapore), Chuanyou Li (Institute of Genetics and Developmental Biology, Chinese Academy of Sciences), Susheng Song (Capital Normal University, China), and Sheliang Wang (Huazhong Agricultural University, China) for providing *Arabidopsis* mutants.

Author contributions

HZ: conceptualization; SD, HC, YS, and HZ: performing the experiments; SD, XX, LX, CQ, YZ, KY, ML, and HZ: data analysis; HZ and SD: writing the manuscript. All authors read and approved the final manuscript.

Conflict of interest

The authors declare that there is no conflict of interest.

Funding

This work was supported by grants from the National Natural Science Foundation of China (32372802), the Zhejiang Provincial Natural Science Foundation of China (LY20C150002), and the Scientific Research Fund of Zhejiang Provincial Education Department (Y202351654).

Data availability

All data supporting the findings of this study are available within the paper and within its supplementary data.

References

- Abe M, Kobayashi Y, Yamamoto S, Daimon Y, Yamaguchi A, Ikeda Y, Ichinoki H, Notaguchi M, Goto K, Araki T. 2005. FD, a bZIP protein mediating signals from the floral pathway integrator FT at the shoot apex. *Science* **309**, 1052–1056.
- Andrés F, Coupland G. 2012. The genetic basis of flowering responses to seasonal cues. *Nature Reviews. Genetics* **13**, 627–639.
- Aparicio-Fabre R, Guillén G, Loredó M, *et al.* 2013. Common bean (*Phaseolus vulgaris* L.) PvTIFY orchestrates global changes in transcript profile response to jasmonate and phosphorus deficiency. *BMC Plant Biology* **13**, 26.
- Aung K, Lin SI, Wu CC, Huang YT, Su CL, Chiou TJ. 2006. *pho2*, a phosphate overaccumulator, is caused by a nonsense mutation in a microRNA399 target gene. *Plant Physiology* **141**, 1000–1011.
- Bari R, Datt Pant B, Stitt M, Scheible WR. 2006. PHO2, microRNA399, and PHR1 define a phosphate-signaling pathway in plants. *Plant Physiology* **141**, 988–999.
- Berry S, Dean C. 2015. Environmental perception and epigenetic memory: mechanistic insight through FLC. *The Plant Journal* **83**, 133–148.
- Bustos R, Castrillo G, Linhares F, Puga MI, Rubio V, Perez-Perez J, Solano R, Leyva A, Paz-Ares J. 2010. A central regulatory system largely controls transcriptional activation and repression responses to phosphate starvation in *Arabidopsis*. *PLoS Genetics* **6**, e1001102.
- Che J, Yamaji N, Miyaji T, Mitani-Ueno N, Kato Y, Shen RF, Ma JF. 2020. Node-localized transporters of phosphorus essential for seed development in rice. *Plant and Cell Physiology* **61**, 1387–1398.
- Chen Y-F, Li L-Q, Xu Q, Kong Y-H, Wang H, Wu W-H. 2009. The WRKY6 transcription factor modulates PHOSPHATE1 expression in response to low Pi stress in *Arabidopsis*. *The Plant Cell* **21**, 3554–3566.
- Cho L-H, Yoon J, An G. 2017. The control of flowering time by environmental factors. *The Plant Journal* **90**, 708–719.
- Clough SJ, Bent AF. 1998. Floral dip: a simplified method for *Agrobacterium*-mediated transformation of *Arabidopsis thaliana*. *The Plant Journal* **16**, 735–743.
- Corbesier L, Vincent C, Jang S, *et al.* 2007. FT protein movement contributes to long-distance signaling in floral induction of *Arabidopsis*. *Science* **316**, 1030–1033.
- Delhaize E, Randall PJ. 1995. Characterization of a phosphate-accumulator mutant of *Arabidopsis thaliana*. *Plant Physiology* **107**, 207–213.
- Dissanayaka D, Ghahremani M, Siebers M, Wasaki J, Plaxton WC. 2021. Recent insights into the metabolic adaptations of phosphorus-deprived plants. *Journal of Experimental Botany* **72**, 199–223.
- Dong J, Ma G, Sui L, *et al.* 2019. Inositol pyrophosphate InsP8 acts as an intracellular phosphate signal in *Arabidopsis*. *Molecular Plant* **12**, 1463–1473.
- Guo MA, Ruan WY, Li RL, *et al.* 2024. Visualizing plant intracellular inorganic orthophosphate distribution. *Nature Plants* **10**, 315–326.
- Hamburger D, Rezzonico E, MacDonald-Comber Petetot J, Somerville C, Poirier Y. 2002. Identification and characterization of the *Arabidopsis* PHO1 gene involved in phosphate loading to the xylem. *The Plant Cell* **14**, 889–902.
- He K, Du J, Han X, Li H, Kui M, Zhang J, Huang Z, Fu Q, Jiang Y, Hu Y. 2023. PHOSPHATE STARVATION RESPONSE1 (PHR1) interacts with JASMONATE ZIM-DOMAIN (JAZ) and MYC2 to modulate phosphate deficiency-induced jasmonate signaling in *Arabidopsis*. *The Plant Cell* **35**, 2132–2156.
- He L, Zhao M, Wang Y, Gai J, He C. 2013. Phylogeny, structural evolution and functional diversification of the plant PHOSPHATE1 gene family: a focus on *Glycine max*. *BMC Evolutionary Biology* **13**, 103.
- Hu B, Zhu C, Li F, Tang J, Wang Y, Lin A, Liu L, Che R, Chu C. 2011. LEAF TIP NECROSIS1 plays a pivotal role in the regulation of multiple phosphate starvation responses in rice. *Plant Physiology* **156**, 1101–1115.
- Huang TK, Han CL, Lin SI, *et al.* 2013. Identification of downstream components of ubiquitin-conjugating enzyme PHOSPHATE2 by quantitative membrane proteomics in *Arabidopsis* roots. *The Plant Cell* **25**, 4044–4060.

- Huang Y, Sun MM, Ye Q, Wu XQ, Wu WH, Chen YF.** 2017. Abscisic acid modulates seed germination via ABA INSENSITIVE5-mediated PHOSPHATE1. *Plant Physiology* **175**, 1661–1668.
- Huang Y, Wang S, Shi L, Xu F.** 2021. JASMONATE RESISTANT 1 negatively regulates root growth under boron deficiency in *Arabidopsis*. *Journal of Experimental Botany* **72**, 3108–3121.
- Jung J-H, Lee H-J, Ryu Jae Y, Park C-M.** 2016. SPL3/4/5 integrate developmental aging and photoperiodic signals into the FT–FD module in *Arabidopsis* flowering. *Molecular Plant* **9**, 1647–1659.
- Jung J-Y, Ried MK, Hothorn M, Poirier Y.** 2018. Control of plant phosphate homeostasis by inositol pyrophosphates and the SPX domain. *Current Opinion in Biotechnology* **49**, 156–162.
- Khan GA, Vogiatzaki E, Glauser G, Poirier Y.** 2016. Phosphate deficiency induces the jasmonate pathway and enhances resistance to insect herbivory. *Plant Physiology* **171**, 632–644.
- Kim D, Langmead B, Salzberg SL.** 2015. HISAT: a fast spliced aligner with low memory requirements. *Nature Methods* **12**, 357–360.
- Kim DH, Doyle MR, Sung S, Amasino RM.** 2009. Vernalization: winter and the timing of flowering in plants. *Annual Review of Cell and Developmental Biology* **25**, 277–299.
- Kim W, Ahn HJ, Chiou T-J, Ahn JH.** 2011. The role of the miR399–PHO2 module in the regulation of flowering time in response to different ambient temperatures in *Arabidopsis thaliana*. *Molecules and Cells* **32**, 83–88.
- Kinoshita A, Richter R.** 2020. Genetic and molecular basis of floral induction in *Arabidopsis thaliana*. *Journal of Experimental Botany* **71**, 2490–2504.
- Klopfenstein DV, Zhang L, Pedersen BS, et al.** 2018. GOATOOLS: a Python library for Gene Ontology analyses. *Scientific Reports* **8**, 10872.
- Kojima S, Takahashi Y, Kobayashi Y, Monna L, Sasaki T, Araki T, Yano M.** 2002. Hd3a, a rice ortholog of the *Arabidopsis* FT gene, promotes transition to flowering downstream of Hd1 under short-day conditions. *Plant and Cell Physiology* **43**, 1096–1105.
- Kong Y, Wang G, Chen X, Li L, Zhang X, Chen S, He Y, Hong G.** 2021. OsPHR2 modulates phosphate starvation-induced OsMYC2 signalling and resistance to *Xanthomonas oryzae* pv. *oryzae*. *Plant, Cell & Environment* **44**, 3432–3444.
- Lee JH, Ryu HS, Chung KS, Posé D, Kim S, Schmid M, Ahn JH.** 2013. Regulation of temperature-responsive flowering by MADS-box transcription factor repressors. *Science* **342**, 628–632.
- Lee JH, Yoo SJ, Park SH, Hwang I, Lee JS, Ahn JH.** 2007. Role of SVP in the control of flowering time by ambient temperature in *Arabidopsis*. *Genes & Development* **21**, 397–402.
- Li B, Dewey CN.** 2011. RSEM: accurate transcript quantification from RNA-Seq data with or without a reference genome. *BMC Bioinformatics* **12**, 323.
- Li D, Zhang H, Mou M, Chen Y, Xiang S, Chen L, Yu D.** 2019. *Arabidopsis* class II TCP transcription factors integrate with the FT–FD module to control flowering. *Plant Physiology* **181**, 97–111.
- Li S, Ying YH, Secco D, Wang C, Narsai R, Whelan J, Shou HX.** 2017. Molecular interaction between PHO2 and GIGANTEA reveals a new cross-talk between flowering time and phosphate homeostasis in *Oryza sativa*. *Plant, Cell & Environment* **40**, 1487–1499.
- Liu L, Liu C, Hou X, Xi W, Shen L, Tao Z, Wang Y, Yu H.** 2012. FTIP1 is an essential regulator required for florigen transport. *PLoS Biology* **10**, e1001313.
- Liu TY, Huang TK, Tseng CY, Lai YS, Lin SI, Lin WY, Chen JW, Chiou TJ.** 2012. PHO2-dependent degradation of PHO1 modulates phosphate homeostasis in *Arabidopsis*. *The Plant Cell* **24**, 2168–2183.
- Lopez-Arredondo DL, Leyva-Gonzalez MA, Gonzalez-Morales SI, Lopez-Bucio J, Herrera-Estrella L.** 2014. Phosphate nutrition: improving low-phosphate tolerance in crops. *Annual Review of Plant Biology* **65**, 95–123.
- Lu H, Wang F, Wang Y, Lin R, Wang Z, Mao C.** 2023. Molecular mechanisms and genetic improvement of low-phosphorus tolerance in rice. *Plant, Cell & Environment* **46**, 1104–1119.
- Ma B, Zhang L, Gao Q, et al.** 2021. A plasma membrane transporter coordinates phosphate reallocation and grain filling in cereals. *Nature Genetics* **53**, 906–915.
- Madison I, Gillan L, Peace J, Gabrieli F, Van den Broeck L, Jones JL, Sozzani R, Ort D.** 2023. Phosphate starvation: response mechanisms and solutions. *Journal of Experimental Botany* **74**, 6417–6430.
- Menary R, Staden J.** 1976. Effect of phosphorus nutrition and cytokinins on flowering in the tomato, *Lycopersicon esculentum* Mill. *Functional Plant Biology* **3**, 201–205.
- Morcuede R, Bari R, Gibon Y, et al.** 2007. Genome-wide reprogramming of metabolism and regulatory networks of *Arabidopsis* in response to phosphorus. *Plant, Cell & Environment* **30**, 85–112.
- Nguyen NNT, Clua J, Vetal PV, Vuarambon DJ, De Bellis D, Pervent M, Lepetit M, Udvardi M, Valentine AJ, Poirier Y.** 2021. PHO1 family members transport phosphate from infected nodule cells to bacteroids in *Medicago truncatula*. *Plant Physiology* **185**, 196–209.
- Olas JJ, Van Dingenen J, Abel C, Dzialo MA, Feil R, Krapp A, Schlereth A, Wahl V.** 2019. Nitrate acts at the *Arabidopsis thaliana* shoot apical meristem to regulate flowering time. *New Phytologist* **223**, 814–827.
- Pandey BK, Verma L, Prusty A, Singh AP, Bennett MJ, Tyagi AK, Giri J, Mehra P.** 2021. OsJAZ11 regulates phosphate starvation responses in rice. *Planta* **254**, 8.
- Pertea M, Pertea GM, Antonescu CM, Chang TC, Mendell JT, Salzberg SL.** 2015. StringTie enables improved reconstruction of a transcriptome from RNA-seq reads. *Nature Biotechnology* **33**, 290–295.
- Petraglia A, Tomaselli M, Mondoni A, Brancaloni L, Carbognani M.** 2014. Effects of nitrogen and phosphorus supply on growth and flowering phenology of the snowbed forb *Gnaphalium supinum* L. *Flora* **209**, 271–278.
- Poirier Y, Thoma S, Somerville C, Schiefelbein J.** 1991. Mutant of *Arabidopsis* deficient in xylem loading of phosphate. *Plant Physiology* **97**, 1087–1093.
- Puga MI, Mateos I, Charukesi R, et al.** 2014. SPX1 is a phosphate-dependent inhibitor of Phosphate Starvation Response 1 in *Arabidopsis*. *Proceedings of the National Academy of Sciences, USA* **111**, 14947–14952.
- Richter R, Kinoshita A, Vincent C, Martinez-Gallegos R, Gao H, van Driel AD, Hyun Y, Mateos JL, Coupland G.** 2019. Floral regulators FLC and SOC1 directly regulate expression of the B3-type transcription factor TARGET OF FLC AND SVP1 at the *Arabidopsis* shoot apex via antagonistic chromatin modifications. *PLoS Genetics* **15**, e1008065.
- Rossiter RC.** 1978. Phosphorus deficiency and flowering in subterranean clover (*T. subterraneum* L.). *Annals of Botany* **42**, 325–329.
- Rouached H, Stefanovic A, Secco D, Bulak Arpat A, Gout E, Bligny R, Poirier Y.** 2011. Uncoupling phosphate deficiency from its major effects on growth and transcriptome via PHO1 expression in *Arabidopsis*. *The Plant Journal* **65**, 557–570.
- Sanagi M, Aoyama S, Kubo A, et al.** 2021. Low nitrogen conditions accelerate flowering by modulating the phosphorylation state of FLOWERING BHLH 4 in *Arabidopsis*. *Proceedings of the National Academy of Sciences, USA* **118**, e2022942118.
- Sattari SZ, Bouwman AF, Martinez Rodríguez R, Beusen AHW, van Ittersum MK.** 2016. Negative global phosphorus budgets challenge sustainable intensification of grasslands. *Nature Communications* **7**, 10696.
- Searle I, He Y, Turck F, Vincent C, Fornara F, Krober S, Amasino RA, Coupland G.** 2006. The transcription factor FLC confers a flowering response to vernalization by repressing meristem competence and systemic signaling in *Arabidopsis*. *Genes & Development* **20**, 898–912.
- Secco D, Baumann A, Poirier Y.** 2010. Characterization of the rice PHO1 gene family reveals a key role for OsPHO1;2 in phosphate homeostasis and the evolution of a distinct clade in dicotyledons. *Plant Physiology* **152**, 1693–1704.
- Sharma N, Geuten K, Giri BS, Varma A.** 2020. The molecular mechanism of vernalization in *Arabidopsis* and cereals: role of Flowering Locus C and its homologs. *Physiologia Plantarum* **170**, 373–383.

- Shim JS, Kubota A, Imaizumi T.** 2017. Circadian clock and photoperiodic flowering in *Arabidopsis*: CONSTANS is a hub for signal integration. *Plant Physiology* **173**, 5–15.
- Simancas B, Munné-Bosch S.** 2015. Interplay between vitamin E and phosphorus availability in the control of longevity in *Arabidopsis thaliana*. *Annals of Botany* **116**, 511–518.
- Song S, Qi T, Fan M, Zhang X, Gao H, Huang H, Wu D, Guo H, Xie D.** 2013. The bHLH subgroup IIIId factors negatively regulate jasmonate-mediated plant defense and development. *PLoS Genetics* **9**, e1003653.
- Srikanth A, Schmid M.** 2011. Regulation of flowering time: all roads lead to Rome. *Cellular and Molecular Life Sciences* **68**, 2013–2037.
- Staswick PE, Tiryaki I.** 2004. The oxylipin signal jasmonic acid is activated by an enzyme that conjugates it to isoleucine in *Arabidopsis*. *The Plant Cell* **16**, 2117–2127.
- Suárez-López P, Wheatley K, Robson F, Onouchi H, Valverde F, Coupland G.** 2001. CONSTANS mediates between the circadian clock and the control of flowering in *Arabidopsis*. *Nature* **410**, 1116–1120.
- Sun L, Song L, Zhang Y, Zheng Z, Liu D.** 2016. *Arabidopsis* PHL2 and PHR1 act redundantly as the key components of the central regulatory system controlling transcriptional responses to phosphate starvation. *Plant Physiology* **170**, 499–514.
- Tamaki S, Matsuo S, Wong HL, Yokoi S, Shimamoto K.** 2007. Hd3a protein is a mobile flowering signal in rice. *Science* **316**, 1033–1036.
- Valverde F, Mouradov A, Soppe W, Ravenscroft D, Samach A, Coupland G.** 2004. Photoreceptor regulation of CONSTANS protein in photoperiodic flowering. *Science* **303**, 1003–1006.
- Veneklaas EJ, Lambers H, Bragg J, et al.** 2012. Opportunities for improving phosphorus-use efficiency in crop plants. *New Phytologist* **195**, 306–320.
- Vicentini G, Biancucci M, Mineri L, Chirivi D, Giaume F, Miao Y, Kyojuka J, Brambilla V, Betti C, Fornara F.** 2023. Environmental control of rice flowering time. *Plant Communications* **4**, 100610.
- Vogiatzaki E, Baroux C, Jung J-Y, Poirier Y.** 2017. PHO1 exports phosphate from the chalazal seed coat to the embryo in developing *Arabidopsis* seeds. *Current Biology* **27**, 2893–2900.
- Wang F, Deng M, Chen J, et al.** 2020. CASEIN KINASE2-dependent phosphorylation of PHOSPHATE2 fine-tunes phosphate homeostasis in rice. *Plant Physiology* **183**, 250–262.
- Wang H, Li Y, Pan J, Lou D, Hu Y, Yu D.** 2017. The bHLH transcription factors MYC2, MYC3, and MYC4 are required for jasmonate-mediated inhibition of flowering in *Arabidopsis*. *Molecular Plant* **10**, 1461–1464.
- Wang JW.** 2014. Regulation of flowering time by the miR156-mediated age pathway. *Journal of Experimental Botany* **65**, 4723–4730.
- Wang ZR, Straub D, Yang HY, Kania A, Shen JB, Ludewig U, Neumann G.** 2014. The regulatory network of cluster-root function and development in phosphate-deficient white lupin (*Lupinus albus*) identified by transcriptome sequencing. *Physiologia Plantarum* **151**, 323–338.
- Wasternack C, Song S.** 2017. Jasmonates: biosynthesis, metabolism, and signaling by proteins activating and repressing transcription. *Journal of Experimental Botany* **68**, 1303–1321.
- Wege S, Khan GA, Jung JY, Vogiatzaki E, Pradervand S, Aller I, Meyer AJ, Poirier Y.** 2016. The EXS domain of PHO1 participates in the response of shoots to phosphate deficiency via a root-to-shoot signal. *Plant Physiology* **170**, 385–400.
- Wild R, Gerasimaite R, Jung JY, et al.** 2016. Control of eukaryotic phosphate homeostasis by inositol polyphosphate sensor domains. *Science* **352**, 986–990.
- Xiao X, Zhang J, Satheesh V, et al.** 2022. SHORT-ROOT stabilizes PHOSPHATE1 to regulate phosphate allocation in *Arabidopsis*. *Nature Plants* **8**, 1074–1081.
- Xu XR, Xu JY, Yuan C, Chen QQ, Liu QG, Wang XM, Qin C.** 2022. BBX17 interacts with CO and negatively regulates flowering time in *Arabidopsis thaliana*. *Plant and Cell Physiology* **63**, 401–409.
- Ye T, Li Y, Zhang J, Hou W, Zhou W, Lu J, Xing Y, Li X.** 2019. Nitrogen, phosphorus, and potassium fertilization affects the flowering time of rice (*Oryza sativa* L.). *Global Ecology and Conservation* **20**, e00753.
- Zarei A, Körbes AP, Younessi P, Montiel G, Champion A, Memelink J.** 2011. Two GCC boxes and AP2/ERF-domain transcription factor ORA59 in jasmonate/ethylene-mediated activation of the PDF1.2 promoter in *Arabidopsis*. *Plant Molecular Biology* **75**, 321–331.
- Zeng H, Wu H, Wang G, Dai S, Zhu Q, Chen H, Yi K, Du L.** 2022. *Arabidopsis* CAMTA3/SR1 is involved in drought stress tolerance and ABA signaling. *Plant Science* **319**, 111250.
- Zeng HQ, Wang GP, Zhang YQ, Hu XY, Pi EX, Zhu YY, Wang HZ, Du LQ.** 2016. Genome-wide identification of phosphate-deficiency-responsive genes in soybean roots by high-throughput sequencing. *Plant and Soil* **398**, 207–227.
- Zeng H, Xia C, Zhang C, Chen L-Q.** 2018a. A simplified hydroponic culture of *Arabidopsis*. *Bio-Protocol* **8**, e3121.
- Zeng H, Zhang X, Zhang X, Pi E, Xiao L, Zhu Y.** 2018b. Early transcriptomic response to phosphate deprivation in soybean leaves as revealed by RNA-sequencing. *International Journal of Molecular Sciences* **19**, 2145.
- Zhai Q, Zhang X, Wu F, Feng H, Deng L, Xu L, Zhang M, Wang Q, Li C.** 2015. Transcriptional mechanism of jasmonate receptor COI1-mediated delay of flowering time in *Arabidopsis*. *The Plant Cell* **27**, 2814–2828.
- Zhang S, Liu Y, Du M, Shou G, Wang Z, Xu G.** 2022. Nitrogen as a regulator for flowering time in plant. *Plant and Soil* **480**, 1–29.
- Zhao L, Li X, Chen W, Xu Z, Chen M, Wang H, Yu D.** 2022. The emerging role of jasmonate in the control of flowering time. *Journal of Experimental Botany* **73**, 11–21.
- Zhao P, You Q, Lei M.** 2019. A CRISPR/Cas9 deletion into the phosphate transporter SIPHO1;1 reveals its role in phosphate nutrition of tomato seedlings. *Physiologia Plantarum* **167**, 556–563.
- Zhu Y, Liu L, Shen L, Yu H.** 2016. NaKR1 regulates long-distance movement of FLOWERING LOCUS T in *Arabidopsis*. *Nature Plants* **2**, 16075.
- Zimmerli C, Ribot C, Vavasseur A, Bauer H, Hedrich R, Poirier Y.** 2012. PHO1 expression in guard cells mediates the stomatal response to abscisic acid in *Arabidopsis*. *The Plant Journal* **72**, 199–211.